ANALYTICAL APPLICATIONS OF CIRCULAR

DICHROISM: USE OF COLOR INDUCTION

REACTIONS FOR QUALITATIVE AND

QUANTITATIVE ANALYSIS

ALLAN RAY ENGLE

Bachelor of Science
Northwestern Oklahoma State University
Alva, Oklahoma
1981

Bachelor of Arts
Southwestern Oklahoma State University
Weatherford, Oklahoma
1987

Master of Science
Oklahoma State University
Stillwater, Oklahoma
1990

Submitted to the Faculty of the
Graduate College of the
Oklahoma State University
in partial fulfillment of
the requirements for
the Degree of
DOCTOR OF PHILOSOPHY
July 1994

ANALYTICAL APPLICATIONS OF CIRCULAR DICHROISM: USE OF COLOR INDUCTION REACTIONS FOR QUALITATIVE AND QUANTITATIVE ANALYSIS
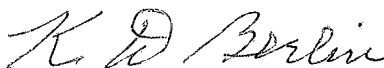
Thesis Approved:

_____

Thesis Adviser

_____

_____

_____

Dean of the Graduate College

PREFACE

Circular Dichroism (CD) spectropolarimetry is a versatile analytical tool. It offers selective detection that has found broad use in a variety of analytical applications, both quantitative and qualitative.This study includes application of CD to three analytical problems that at first glance are seemingly unrelated. They do, in fact, have a common thread in that they are potential candidates for CD analyses via a color induction reaction. It is hoped that continued development of analytical applications for CD involving a diverse array of analytical problems such as these will help dispel the belief that CD is useful only as a tool for stereochemical structure elucidation. Furthermore, it is hoped that CD as an analytical technique can be elevated to a position equal to that of other primary analytical methods and spur additional research and development for instrumentation and analytical applications.

I would like to take this opportunity to recognize several people who have served as a source of inspiration during my graduate studies. I'm quite sure that, if not for Dr. Ken Brown of NWOSU and Drs. Dan Dill, Don Hertzler, Bobby Gunter, and Harold White of SWOSU, I would not have chosen to pursue graduate studies in chemistry. In addition to being fine teachers and chemists, they are human beings without peer. Mr. Jodee d'Avignon has been my good friend for a number of years and deserves much of the credit for my initial interest in pursuing science as a career.

TABLE OF CONTENTS

LIST OF TABLES

LIST OF FIGURES

x

CHAPTER I

CIRCULAR DICHROISM AS AN ANALYTICAL TOOL

The use of circular dichroism (CD) as a means for the study of molecular stereochemistry is well documented. There are numerous examples of how CD has been used to extract information from chiral organic molecules and how this information has been used to determine relative and, in some cases, absolute configurations.[1] However, many would say that the analytical applications of CD have not been as thoroughly investigated. It is often the case that analytical determinations can be accomplished only after complete chromatographic separation or when a detector is employed that is selective enough to differentiate the analyte from the host of possible interfering substances. Because of its selectivity, CD can deliver a powerful, yet elegant, method for the determination of enantiomeric purities of chiral compounds. In a traditional analytical setting, CD can allow for determinations in the analysis of unresolved complex mixtures in forensic, clinical, and pharmaceutical samples.[2] Additional examples of the versatility of CD include its use for calculating formation constants and monitoring intermediates in biosynthetic pathways.

Simply put, CD is a modified form of absorption spectrophotometry that uses circularly polarized light to measure an absorption difference. CD

is a selective method of detection with specific molecular requirements; that is, the analytes must possess both a chiral center and an associated chromophore. These specific molecular requirements make it an ideal selective detector for drug molecules and certain natural products. Additionally, there are several other analytical advantages to CD. Compounds with broad, featureless absorption bands can have CD spectra with both positive and negative inflections and crossover points at which the CD signal is zero. Since CD measures the difference in absorption, a compound with a weak absorption band can have a relatively strong CD signal. In combination with readily obtainable data reduction and analysis computer software, full spectrum CD can provide a wealth of qualitative and quantitative information. In some instances, one of the molecular requirements may be missing or attenuated. If the chromophore is the deficient molecular requirement, the value of the CD detector may be extended by adding a chromophore through the use of either a chromogenic reaction or by complexation. On the other hand, a weak chiral signal can be enhanced, for example, via chiral induction by complexing the analyte with another chiral moiety. This CD induction is an important recurring theme, particularly as it relates to selectivity. Modification of the chiral environment has been shown to be one of the most important recent developments in relation to improving the ability of CD to discriminate between enantiomers and diastereoisomers in mixtures.[1]

CHAPTER II

HISTORICAL AND THEORETICAL CONSIDERATIONS

History of Optical Activity

In the early 1800s, descriptions of those phenomena that govern modern chiroptical techniques began to appear. In 1808, Malus reported that a beam of light became polarized when passed through a crystal of Iceland spar.[3,4] Three years later, the first recorded observation of optical activity was made by Arago. With the use of a quartz plate, he was able to rotate the plane of polarization of plane-polarized light.[4] Shortly thereafter, Biot was able to demonstrate that optical activity was not limited to crystalline materials, but was also a property of solutions of certain natural products.[5] Such measurement of optical rotation at a specific wavelength is termed polarimetry. During the same time period, Biot and Fresnel independently observed that as the wavelength of light incident upon the sample decreases, the angle of rotation in the plane of plane-polarized light increases. This phenomenon is now referred to as optical rotatory dispersion (ORD) and can be described as polarimetry at several wavelengths.[6] Another very important observation was made by Haidinger in 1847 as he studied the unequal absorption of circularly polarized light by amethyst quartz, a phenomenon that is now known as CD. Much as Biot was able to show that optical activity was not limited to crystalline

materials, in 1896 Amie Cotton first observed CD in solution when light from a sodium flame was passed through a solution of potassium chromium tartrate. It was from this experiment that Cotton was able to suggest that the phenomenon of circular dichroism was in fact due to the unequal absorption of the left and right circularly polarized components of plane-polarized light.[4]

Louis Pasteur, in 1848, provided a key piece of information regarding the physical basis of optical activity when he described sodium ammonium tartrate crystals as a racemic mixture. He was able to mechanically resolve the racemate and prepare solutions of each enantiomer. For each solution, he noted that the plane of polarization was rotated through an angle equal in magnitude but opposite in sign. Pasteur then reasoned that the macroscopic asymmetry of the crystal was a reflection of the molecular geometry.[4] He concluded that for a molecule to show optical activity it had to exist in two nonsuperimposable mirror image forms.[7] Through his study of the tartrate crystals, Pasteur was able to intuitively conceptualize the tetrahedral carbon atom.[5] The idea of an asymmetric carbon atom was advanced in 1874 by Van't Hoff and Le Bel who proposed the tetrahedral and square pyramid geometries respectively. The eventual acceptance of Van't Hoff's tetrahedral geometry is the basis of current three dimensional molecular descriptions, or more specifically, the concept of chirality.[8]

Historical developments to this point provide the operational basis for the three most common chiroptical methods: polarimetry, ORD, and CD. Of

these three, ORD and CD provide the most detailed information that can be used for characterization purposes. In a typical ORD spectrum (Figure 1b), two distinct regions can be identified. As the spectrum is scanned from longer to shorter wavelengths, the optical rotation increases monotonically. This portion of the ORD curve is commonly referred to as a plain curve. Beyond this point, over the range of an absorption band, the spectrum exhibits one or more irregularities. The measured rotation can show a peak, followed by a rapid inflection to a trough of opposite sign, followed by a gradual return to the plain curve spectrum, or the irregularities can follow the same sequence of events but in reverse order. This part of the ORD spectrum is referred to as an anomalous curve and is due to the Cotton effect, which is the combined result of differential absorption and unequal
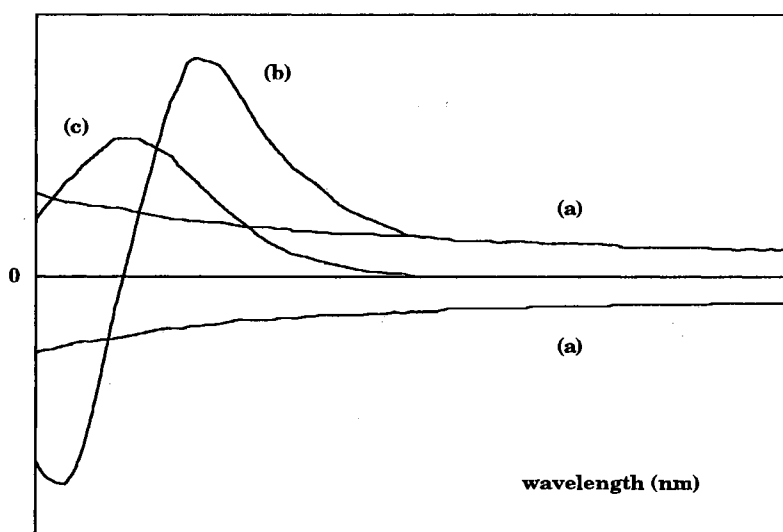
Figure 1. Typical chiroptical spectra: a) plain ORD curves, b) anomalous ORD curve with a single Cotton effect, and c) CD curve with a single positive Cotton effect.

transmission velocities of the left and right circularly polarized light.[9] CD spectra also exhibit the Cotton effect. Although ORD may provide more spectral information, certain anomalies from background effects may appear. These can be caused by the rotational contributions of outlying absorption bands from the same chromophore, other chromophores, and at very short wavelengths, effects from $\sigma \rightarrow \sigma^*$ transitions. Such events are not desirable from an analytical viewpoint and are not present in the CD spectrum. The Cotton effect in a simple CD spectrum appears as a single positive or negative maximum (Figure 1c).

In 1896, Drude postulated what was to be the first theory on ORD.[9] Drude proposed that any charged particle moving through a disymmetric molecular structure would be forced to move in a helical pattern.[4] Optical activity, therefore, was described by Drude as the result of interactions between the electronic environment of the medium and the original electromagnetic wave.[10] By 1916, Gray[5] had developed a theory that attempted to relate the physical arguments of Drude's theory with the geometrical models of optical activity proposed by Pasteur, Le Bel, and Van't Hoff, which retained the tetrahedral model of Van't Hoff. Born and Oseen offered further refinements of this idea.[5]

Mathematical treatments of the above theories were all based upon classical assumptions. Although there have been attempts to interpret optical activity by application of quantum mechanical theory, including work by Rosenfeld, Condon, and others, there is still not a single

comprehensive theory that will allow for accurate prediction of the

magnitude and sign of chiroptical phenomena associated with molecular

structures.[5]

<p align="center">Theory of Chiroptical Measurements</p>

All three chiroptical techniques, polarimetry, ORD, and CD, are

based on the interaction of polarized light with a chiral species. In general,

for spectroscopic techniques such as ultraviolet-visible spectrometry,

monochromatic light incident upon the sample can be described by a

number of transverse waves (Figure 2). Each wave has associated with it

time dependent electric and magnetic fields that are oriented at right

angles to one another and orthogonal to the direction of propagation.
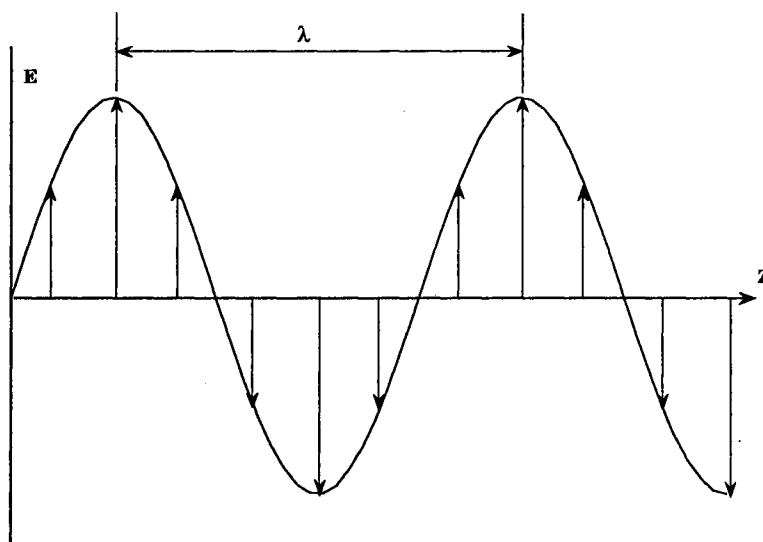
Figure 2. Transverse wave representation of the electric field associated
with a monochromatic light beam. The arrows represent the magnitude of
the oscillating electric field. The distance between cycles is the wavelength,
λ, of the radiation.

In chiroptical photometry, the monochromatic linearly polarized incident light is described by a transverse wave whose electric field is limited to oscillation in one direction only. For the purposes of this discussion, the associated magnetic field may be ignored. Linearly polarized light can be expressed as the vector sum of two circularly polarized beams. A view of either circularly polarized beam along the axis of propagation (z-axis) would have a circular appearance as a function of time, while a view from the x or y direction would show the electric field vectors tracing a left- or right-handed helix as the respective vectors rotate counterclockwise or clockwise (Figure 3). In comparison, a view down the axis of propagation of a linearly polarized beam has the appearance of a single line oriented in the plane of polarization.
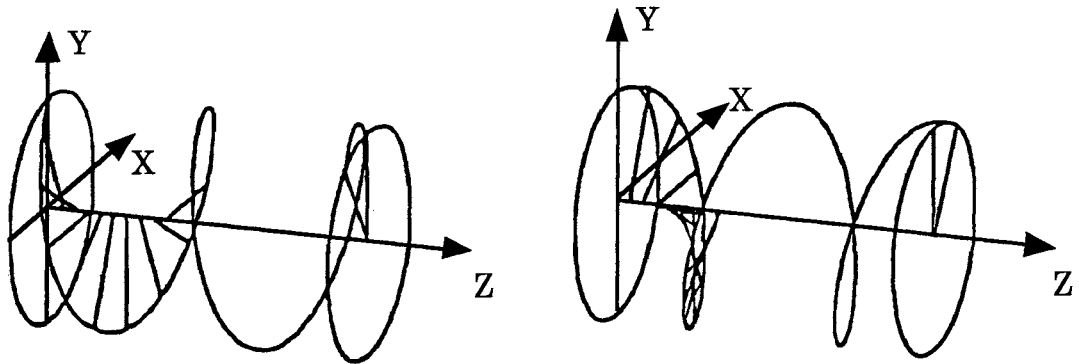
Figure 3. Vector diagram of right and left circularly polarized light: right circularly polarized light (on the left) and left circularly polarized light (on the right). Diagram represents a trace of the ends of the electric field vectors during propagation. (adapted from reference 11)

When a monochromatic, linearly polarized beam is passed through an achiral sample, the circularly polarized electric field vectors remain in phase with each other (Figure 4a). As a result, the angles between each vector and the original plane of polarization remain equal ($\omega = \omega'$), and the beam, upon exiting the sample, remains linearly polarized and in the same plane of polarization as the incident beam. When the sample is chiral, the refractive indices are different for rays of left and right circular polarized light. Since the speed of the respective left and right circular polarized beams is a function of the index of refraction for each, one beam becomes retarded relative to the other. The transmitted beams are then out-of-phase ($\omega \neq \omega'$), but still equal in intensity (Figure 4b). The resulting vector is said

(a)   (b)
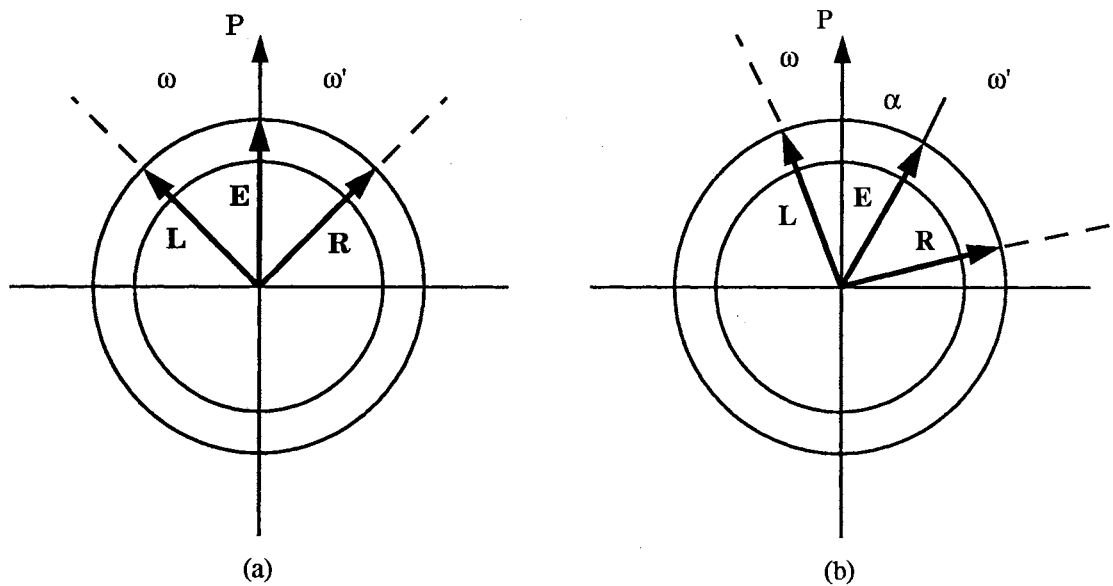
Figure 4. Electric field vectors emerging from a) an achiral medium and b) a chiral medium. P is the original plane of polarization, L and R are the left and right circularly polarized electric field vectors, and E is the resultant electric field vector.

to be polarized, but it is then rotated through an angle α relative to the direction of the original plane of polarization.[7]

For a sample solution with a 10 cm path length, this optical rotation, α, at a given wavelength, λ, is defined by the Fresnel equation

$$\alpha = \frac{1800}{\lambda}\left(\eta_L - \eta_R\right) \tag{1}$$

where α is measured in degrees/dm, and η_L and η_R are the indices of refraction for the left and right circularly polarized beams.[6] The medium that exhibits this phenomenon of different indices of refraction for left and right circularly polarized light is said to be optically active and the material itself is circularly birefringent.[7]

In polarimetry, α is usually measured at only a few pre-selected wavelengths. In ORD, the quantity is measured as a function of λ to produce a spectrum. The equation is not comprehensive, especially when applied to solutions, because the index of refraction is a function of the concentration as well as of λ. In order to include this dependence, the optical activity of a substance in solution is more often expressed in terms of the specific rotation, $[\alpha]$,

$$[\alpha] = \frac{\alpha}{c \times b} \tag{2}$$

where c is the concentration in g/mL and b is the path length in dm.

In order to compare rotations among solutions of different materials, another quantity, the molar rotation, $[\Phi]$, is introduced.

$$[\Phi] = \frac{[\alpha]M}{100} \tag{3}$$

In this equation, $[\alpha]$ is the specific rotation, M is the molecular weight of the compound in g/mole, and the numerical constant is a scaling factor.[6,11]

In addition to circular birefringence, a chiral substance may show significant differential absorption between the left and right circularly polarized components of the linearly polarized beam;[7] i.e., CD. The absorbances for the two components by a chiral substance in solution are given by Beer's Law:

$$A_L = \varepsilon_L bc \tag{4}$$

$$A_R = \varepsilon_R bc \tag{5}$$

where the subscripts refer to the left and right circularly polarized components, and ε_L and ε_R are the molar absorptivities. In the practice of CD, the relationship is expressed as the difference in absorption:

$$\Delta A = \Delta \varepsilon bc \tag{6}$$

The differential absorbance, ΔA, of the two circularly polarized components implies that the magnitudes of their respective electric field vectors, **L** and **R**, are unequal. Along the axis of propagation (z axis), the

polarization is now elliptical because the resultant vector, **E**, no longer oscillates in a single plane.[4] CD measurements, therefore, can be expressed either in terms of the difference in absorption or in terms of an ellipticity, ψ, which is a measure of the eccentricity of the ellipse. The ellipticity of the transmitted light beam is defined mathematically as the arctangent of the ratio of the minor axis of the ellipse, **OA**, to the major axis of the ellipse, **OB** (Figure 5).

Figure 5. Production of elliptically polarized light in CD. P is the original direction of polarization, **L** and **R** are left and right circularly polarized light respectively, and **E** is the resulting electric field that is now elliptically polarized.

$$\psi = \tan^{-1} \frac{\mathbf{OA}}{\mathbf{OB}} \tag{7}$$

This relationship is a general one and is independent of the phase of the material because the origin of the elliptical polarization is ΔA. Since CD measurements are made primarily on chiral materials in solution, for the purposes of this discussion, relationships are based on the proportional normalized quantity, $\Delta \mathcal{E}$.

The ellipticity is related to the difference in the molar absorptivities, $\mathcal{E}_L$ and $\mathcal{E}_R$, to a good approximation in the following way. If a_O is the amplitude of the circular components incident upon the sample, and a_L and a_R respectively are the amplitudes of the circular components after emerging from the sample, then the molar absorptivities are related to the ratios of the respective amplitudes by the following equations:

$$\frac{a_L}{a_O} = e^{-2\pi b \kappa_L / \lambda} \tag{8}$$

$$\frac{a_R}{a_O} = e^{-2\pi b \kappa_R / \lambda} \tag{9}$$

where κ is the absorption index and will be defined later.

Defining the minor axis, **OA**, as the difference in the amplitudes

$$\mathbf{OA} = a_R - a_L \tag{10}$$

and **OB** as the sum of the amplitudes,

$$\mathbf{OB} = a_R + a_L \tag{11}$$

substituting these relationships into (7) gives

$$\tan \psi = \frac{a_R - a_L}{a_R + a_L} \tag{12}$$

With the appropriate substitutions of equations (8) and (9) and rearrangement, the ellipticity can be expressed in terms of the absorption indices, κ.

$$\tan \psi = \frac{1 - e^{-\left(2\pi(\kappa_L - \kappa_R)b\right)/\lambda}}{1 + e^{-\left(2\pi(\kappa_L - \kappa_R)b\right)/\lambda}} \tag{13}$$

At small values of x, $(1 - e^{-x})$ is approximately equal to x, so

$$\tan \psi = \frac{\left(2\pi(\kappa_L - \kappa_R)b\right)/\lambda}{2 - \left(\left(2\pi(\kappa_L - \kappa_R)b\right)/\lambda\right)} \tag{14}$$

Assuming κ_L-$\kappa_R \ll 2$, then

$$\tan \psi = \frac{\pi b}{\lambda}\left(\kappa_L - \kappa_R\right) \tag{15}$$

For small ellipticity values, $\tan \psi$ is approximately equal to ψ, and the above equation reduces to

$$\psi = \frac{\pi b}{\lambda}\left(\kappa_L - \kappa_R\right) \tag{16}$$

The more modern and preferred unit of molar absorptivity, $\mathcal{E}$, has since replaced the absorption index, κ.[12] The relationship between these two constants is expressed by the following equation:[4]

$$\kappa = \frac{\varepsilon\, c\, \lambda}{4\,\pi \log_{10} e} \tag{17}$$

Making the appropriate substitutions for κ_L and κ_R into (17) gives equation (18)

$$\psi = \frac{b\, c}{4 \log_{10} e}(\varepsilon_L - \varepsilon_R) \tag{18}$$

for the ellipticity in radians. It should be noted that this is a calculated ellipticity value and should not be confused with the measured ellipticity, which uses concentration units of g/cm^3.[11] The degree is the customary unit used to express values of measured ellipticity. Multiplying the above equation by the appropriate conversion factor of $180/\pi$ gives the final relationship

$$\psi = 32.98\, c\, b\left(\varepsilon_L - \varepsilon_R\right) \tag{19}$$

When this is normalized by dividing by concentration and path length, the quantity that is referred to as the molar ellipticity is obtained with the units of degree·liter/mole·cm.

$$[\theta] = 32.98 \left(\varepsilon_L - \varepsilon_R \right) \tag{20}$$

Converting these units to degree cm2/decimole yields the expression most commonly encountered in the earliest literature

$$[\theta] = 3300 \left(\varepsilon_L - \varepsilon_R \right) \tag{21}$$

This expression equates the molar ellipticity to the change in molar absorptivity at a given wavelength. Although ε_L and ε_R are typically unequal over the range of the entire absorption band, they reach their maximum differential near the absorption maximum for the chromophore.[5] This difference[4] is on the order of 10^{-2} to 10^{-3} absorbance units and offers evidence of why a measurable CD signal seemingly occurs only near the wavelength region of an absorption maximum.[5]

All currently produced commercial CD spectropolarimeters measure the difference in absorbance as opposed to the ellipticity, although they are calibrated to a scale of millidegrees as a result of historical precedent. In order to more easily use CD as an analytical tool, we have chosen to define the molar ellipticity, θ_M, in a manner that makes it analogous to the proportionality constant in the Beer-Lambert expression:

$$\theta_M = \frac{\psi}{b \, c} \tag{22}$$

In this case, ψ is the measured ellipticity in degrees, c is the concentration in moles/L, and b is the path length in cm. This method of

defining the molar ellipticity causes our values for molar ellipticity to be two orders of magnitude different from those reported in the literature.

CHAPTER III

INSTRUMENTATION

Description of Instrument

All CD and UV measurements were made with a JASCO (Japan Spectroscopic Co., Ltd.) model J-500A automatic recording spectropolarimeter. The light source for this instrument is a 450 watt xenon arc lamp. The lamp is operated under an inert atmosphere of nitrogen gas to protect the optical system from ozone damage. The spectropolarimeter is interfaced to an IBM compatible microcomputer through the JASCO IF-500 II serial interface unit; the computer drives the instrument and provides data processing capabilities. Spectra were exported as ASCII files for subsequent import into commercial data analysis and plotting software.

The instrument was calibrated daily with a 0.025% (w/v) solution of androsterone in dioxane as recommended by JASCO.[13] Sensitivity, number of scans per measurement, and slit width were optimized to provide the minimum acquisition time necessary without adversely affecting the quality of the spectra.

J-500A Optical System

The optical system of the JASCO J-500A closely resembles that of a conventional single beam UV-visible spectrophotometer, with the necessary

modifications added to produce the circularly polarized monochromatic radiation needed for CD measurements. The optical system is shown schematically in Figure 6.
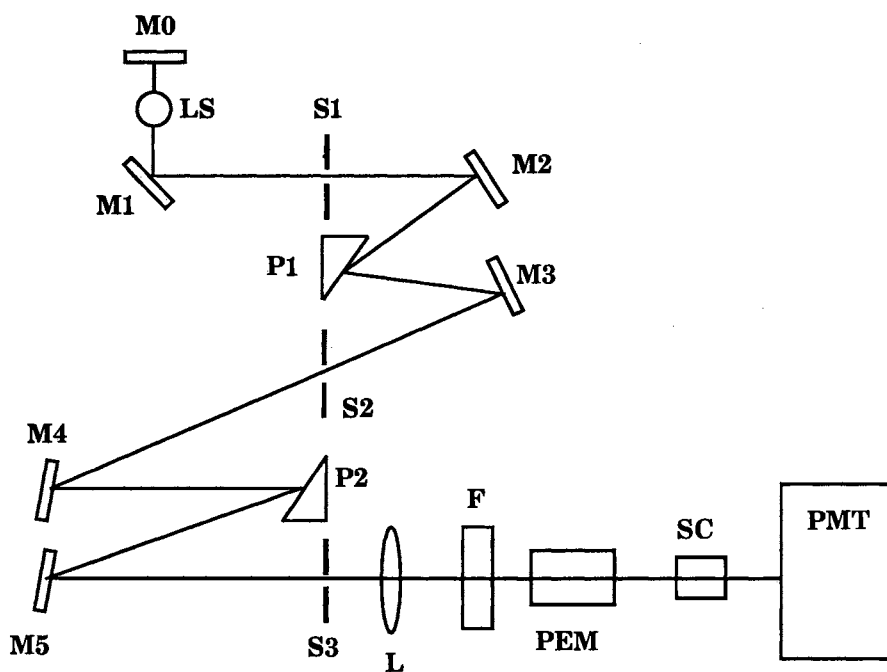
Legend: M0, M1, M2, M3, M4, M5: spherical mirrors
LS: light source
S, S2, S3: slits
P1: first prism (horizontal axis)
P2: second prism (vertical axis)
L: lens
F: filter
PEM: photoelastic modulator (piezoelectric)
SC: sample cell
PMT: photomultiplier tube

Figure 6: Optical system for the J-500A spectropolarimeter (adapted from reference 13).

The light beam is focused onto the entrance slit, S1, by the mirror M1. Two identical monochromators are located between slits S1 and S3 and are separated by slit S2. The prisms P1 and P2 have dual functions as dispersion elements and birefringence polarizers. Light emerging from P2 is linearly polarized monochromatic light. Lens L focuses this light onto filter F, which serves to remove any unpolarized light. PEM is a piezoelectric modulator that converts the linearly polarized light to circularly polarized light. The circularly polarized light passes through the sample chamber and onto the detector, which is a high gain photomultiplier tube operated at constant current.

In practice, the CD spectrum is obtained by calculating the difference in the absorbance, ΔA , for the left and right circularly polarized beams. Since the molar ellipticity for a solution, $\Delta \mathcal{E}$, amounts to a very small difference, typically on the order of 10^{-2} to 10^{-3} between two relatively large numbers, direct measurement of the intensities of the transmitted beams of the left and right circularly polarized components does not provide a good means for measurement of the circular dichroism. Instead, JASCO engineers have chosen to measure alternately the intensities of the transmitted beams as direct and alternating signals using photomultiplier output voltages as described below.

As described previously, the device employed to produce the circularly polarized light is a PEM. It is designed to produce left and right beams of circularly polarized light in an alternating fashion at a frequency

of 50 KHz. This is superimposed on a constant DC signal voltage that represents the average of the left and right circularly polarized beams. Upon passage through the sample, the two beams experience differential absorption. This causes the intensity of the transmitted light to vary as in Figure 7. The positive and negative maxima correspond to the intensities of the right or left circularly polarized light beams, I_R and I_L, which are a function of the relative magnitudes of $\mathcal{E}_R$ and $\mathcal{E}_L$. The CD value is calculated directly by the measurement of the voltage at the photomultiplier tube proportional to the average intensity, I_A, and the voltage representing the amplitude of the AC signal, S.[13]
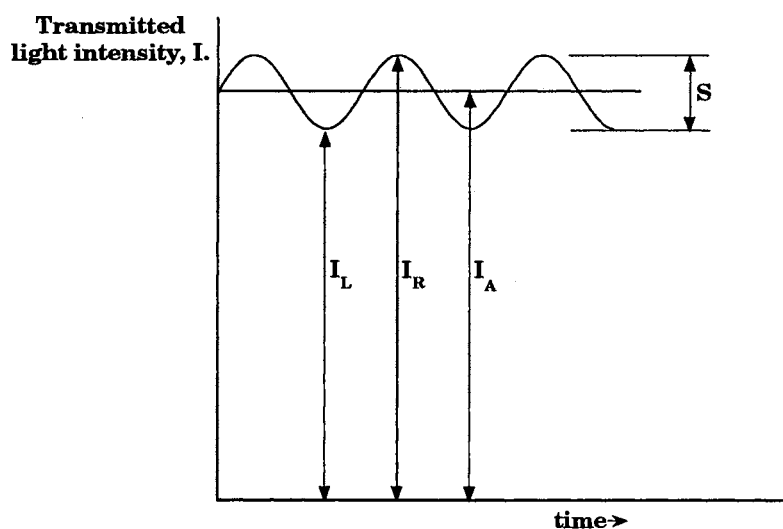
Figure 7. Relationship of AC carrier wave to CD signal.

CHAPTER IV

USE OF INDUCED CIRCULAR DICHROISM FOR OPTICAL PURITY
DETERMINATIONS

Introduction

Perhaps the most visible examples of the relationship between
stereoisomerism and physiological activity were the teratogenic effects
produced by S-(-)-thalidomide in the 1960s.[14] Although the existence of these
so called structure activity relationships (SAR's) have been known for over
a century, this tragedy initiated an increased awareness of chirality and its
pharmacological consequences that has now spread throughout the
pharmaceutical industry and beyond. As chiral technology comes of age,
there is an increased thrust in the drug industry to use the improved
methods for synthesis and isolation to produce new drug substances as
single enantiomers and to effect what has been coined "racemic switches."
These racemic switches employ chemistries for redevelopment of single
enantiomeric formulations from older preparations that were originally
marketed as racemates. According to Ariëns,[15] in most instances, it makes
little sense to develop or market a racemic formulation. Indeed,
pharmacokinetic data collected through clinical trials using racemic drugs
have been referred to as "pharmacokinetic nonsense," due to the possibility
of the enantiomeric forms having different pharmacological effects.[15]

These events, as they are associated with production of enantiomeric formulations, have caused the Food and Drug Administration (FDA) to respond with a policy statement concerning chiral drugs. Prior to revisions of the guidelines for new drug applications, there were no formal rules concerning development of drug substances for which the possibility of stereoisomerism existed. Before the advent of chiral stationary phases for high-performance liquid chromatography (HPLC) in the late 1970s, any efforts to determine the safety or efficacy of a particular drug substance were confined to those drugs for which an economic stereospecific synthetic route was available.

Current FDA guidelines for new drug applications are very clear concerning the question of stereochemistry. Under these regulations, all methods used in the manufacture of the drug must be specified, including tests to verify its identity, strength, and purity. The molecular structure of the drug must be shown, along with identification of all chiral centers, if present, and the enantiomeric ratio.[16]

Analytical methodologies to verify identity and determine purity must be continually developed and refined in order to satisfy FDA regulations. The determination of diastereoisomers that are components of a binary mixture is relatively simple by virtue of the different chemical and physical properties of the isomers. Conversely, the accurate determination of a mixture of enantiomers is a much more difficult problem. The determination can be accomplished only when complete chromatographic

separation of the isomers is possible or when a detector is used that is capable of discriminating between the enantiomers without a prior separation step.

Many procedures that have been used to determine the enantiomeric ratio rely on the ability to resolve a mixture of enantiomers. Pasteur was credited as the first person to effect an enantiomeric separation. He was fortunate in that the mixture he sought to resolve, tartaric acid, was composed of *individual* crystals of the optically pure tartrates. A case that is far more common is the racemic compound, in which the individual crystals are composed of a mixture of the two isomers, making mechanical separations impossible.[16] Accordingly, one must turn to the more sophisticated methods that involve chiroptical measurements and/or chromatography. Methods most often cited in the literature use NMR, gas chromatography (GC), supercritical fluid chromatography (SFC), HPLC, or micellular electrokinetic chromatography (MEK).[17] In general, the methods used to measure enantiomeric ratios (ER) require two independent measurements to be made, often with two different detectors. The independent measurements are usually predicated on the formation of diastereoisomeric intermediates that have different chemical shifts, spectra, retention times, etc.

HPLC methods have been the most extensively studied. A review of the literature reveals three general approaches to ER determinations that use HPLC. In the first, a chiral stationary phase column is used for the

formation of diastereoisomers leading to the direct separation of enantiomers. The second method utilizes an achiral column with certain chiral mobile phase additives to effect separation.[8] The third method of ER determination also utilizes an achiral column, but in this case, diastereoisomers are not formed. The enantiomers are co-eluted and a combination of detectors are used to produce the two necessary independent measurements. The two detectors typically include a chiroptical detector, such as polarimetry, along with either absorption spectrophotometry or a refractive index detector.[18] Interrogation of the sample by two detectors produces the two necessary independent measurements.

Those methods that employ chromatography for the exact determination of ERs may fall short of an accurate determination for a number of reasons. Chromatographic procedures are influenced by band spreading and overlap, changes in elution order, and on-column racemization.[19] Long retention times are often the norm, especially in HPLC, although very reasonable times of a few seconds to several minutes have been reported for MEK and SFC methods.[20,21] Additional difficulties relate to production of a measurable signal for detection. Because pathlengths are very short, it may be necessary to try to compensate for this by increasing the injection concentration. Columns are, however, easily overloaded when injection concentrations are increased. As an alternative to increasing the injection concentration, a more intense illumination source may be used in an effort to enhance the signal. Laser illumination

has been used as a replacement for conventional sources, but it has been problematic in terms of noise and instability.[17,22] Problems with detection are exacerbated if CD or polarimetry detectors are used.[23] Another concern is that if single channel detection is used the opportunity to achieve selectivity is lost. Thus, many factors contribute to the difficulty in attaining a high level of precision in ER determinations.

Even the best of these methods are challenged when used in the determination of the ER for a mixture that lies in the mole fraction range of $x > 0.95$. Armstrong[24] has discussed use of post column chiroptical detectors such as CD and polarimetry for liquid chromatography using chiral stationary phases as well as conventional columns with two detector systems. He has conservatively estimated the relative error in the determination of the ER for a 99:1 admixture of enantiomers using HPLC with a conventional column in two detector mode to be on the order of 200%. It is not unusual for the errors associated with the minor component to be large compared to the major component, although with chiroptical detectors this situation occurs because of the small absolute signal or signal difference to be measured and the accompanying poor signal to noise ratio.[24]

One priority of this study was to decrease the imprecision of the ER determination for an admixture at the limit of approximately 99:1. In order to accomplish this, a color derivatization reaction was utilized to shift the CD spectrum away from the UV and the many potential absorbing

interferences that could seriously hamper background limited detection techniques such as CD. Moreover, it was important to develop a method that would utilize the primary advantage that full spectrum CD detection has over its counterpart as a single wavelength detector in HPLC, namely that of selectivity.

The selectivity advantages that CD possesses make it an ideal detector for the routine direct determination of ERs in unseparated bulk samples.[2,23] Two common methodologies for this type of determination have been investigated. The simpler of the two cases is based on the measurement of the net CD and the total absorbance signal for the admixture.

Since CD spectra for enantiomers are mirror images of each other, the net CD signal is proportional to the difference in the enantiomer concentrations (23), while the absorbance signal is proportional to the sum of the enantiomer concentrations (24):

$$\psi = b\left(\theta_L C_L - \theta_D C_D\right) \tag{23}$$

$$A = b\left(\varepsilon_L C_L + \varepsilon_D C_D\right) \tag{24}$$

where D and L refer to the respective enantiomers.

The ER is then calculated by the simultaneous solution of equations (23) and (24), which represent the two independent measurements. This

technique has been shown to work well for standard reference materials,[25] but since the total concentration for both isomers is determined by a non-selective detector, such as absorbance, it is sensitive to interfering absorbers that may be difficult to remove. In small amounts, the presence of these interferences would have no effect on the CD measurement but would cause a negative bias when calculating the ER due to a positive bias in the calculation of the total concentration of enantiomers. Clearly, much of the advantage of the selectivity is lost when a non-selective detector is used for measurement of the total concentration.

As an alternative to the two detector approach described above, one can obtain the two unique measurements by making two independent CD measurements.[1] Spectra are obtained for equimolar concentrations of the analyte dissolved in two different solvent systems, one that is chiral (i.e., cyclodextrin modified) and the other that is achiral. The ability of the method to distinguish the enantiomers is a result of the formation of diastereoisomers *in situ* in the chiral solvent system. This approach should alleviate most problems associated with anonymous achiral absorbers by reducing any interferences to those that are CD active. The success of this approach depends on the ability of the chiral solvent system to discriminate the chiral analyte from the interferences in the wavelength range of the measurement. For drug substances and many natural products, this is in the UV range. Since CD spectropolarimetry is a background limited technique, the sum total of absorptions from the analyte and interferences

are often so strong that the CD signal may become lost in the large background absorbance. Under these conditions, it may become necessary to employ a strategy to counteract this problem.

Degrees/dm to the method was sought that uses CD detection for both independent measurements that maintains the selectivity of the detector and simultaneously allows for an increase in measurement precision. In order to retain the inherent selectivity property of the CD detector, a color reaction was employed to move the wavelength of measurement into the visible region thereby avoiding the large background absorbance effects caused by the presence of UV absorbing chromophores. For the second improvement, we sought to increase the precision in the mole fraction range $x = 0.95$ to $x = 1.00$ through the use of measurements made at multiple wavelengths and prediction based on multivariate analysis techniques. An unexpected result of the color reaction was the discovery that it might be possible to reduce the number of experiments necessary to obtain the two independent measurements from two to one.

A variation of the biuret reaction[26] was used as the basis for shifting the wavelength(s) of measurement into the visible and away from the host of possible interfering substance. The biuret reagent was developed for the determination of total serum protein via absorbance detection. It was also used to assay the aminoglycoside antibiotic, neomycin sulfate.[27] The biuret reaction is one of the oldest chemical methods for measuring protein, dating back to 1915.[26] Its name arises from the complexation reaction

between Cu(II) ions in strongly alkaline solution and biuret, which is the condensation product formed when urea is heated. When the Cu(II) ions coordinate with ligand groups associated with peptide chains, a purple colored complex results.[28] Several formulations of the biuret reagent have been used. They vary somewhat in the ratio of copper to ligand and in the type of ligand that is used to prevent the precipitation of copper as the hydroxide. The biuret reagent used in this study was developed using the formulation of Gornal *et al.*[26] as an initial model, although the concentrations of copper, tartrate ion, and hydroxide had to be optimized for this particular system. When prepared with the *l*-enantiomer of tartaric acid, the metal complex is chiral. The specific nature of the chiral-chiral interactions from within the first coordination sphere of the metal-ligand complex lead to electronic transitions that originate from differential absorption of the right and left circularly polarized light. The unequal absorption of the circularly polarized light by the chiral complex results in CD activity in the visible region of the spectrum. Measurements are made with CD as the only detector, and the modified biuret reagent is used as the solvent system.

When an analyte undergoes ligand exchange with a chiral tartrate ion, a situation similar to the cyclodextrin example occurs in that diastereoisomers are formed *in situ*. The resultant mixed complexes have CD spectra that show significant changes from the CD spectrum of the modified biuret reagent. Complexation chemistry is also used in ligand

exchange chromatography where diastereoisomers are formed with immobilized Cu(II) ions as chiral stationary phases for enantiomeric separations.[29] As a model system with which to test the color derivatization combined with CD detection, the four ephedrine isomers were exchanged in binary mixtures with *d-*, *l-*, and *meso*-tartrate complexes of Cu(II).

Experimental

Standard Materials

Ephedrine is the general name given to a family of compounds isolated from members of the genus *Ephedra*. The ephedrines exist as four stereoisomers: *d-* and *l-*ephedrine and *d-* and *l-*pseudoephedrine. The principal naturally occurring forms are *l-*ephedrine and *d-*pseudoephedrine. They have been extracted from the leaves of *Ephedra distachya,*[30] one of a family of shrubs indigenous to northern China, India, and Spain.[31] For the pseudoephedrine enantiomeric pair, only the *d-*isomer elicits the desired physiological response. Because of its therapeutic value as an orally administered sympathomimetic amine, pseudoephedrine is a primary active ingredient in many proprietary drug products. Like most optically pure enantiomers, however, there is the potential for chiral inversion to occur over time with a resulting change in potency. For those compounds with a single chiral center, the process ultimately ends with the formation of the 50:50 racemic mixture.

There are a number of aliases for the four ephedrines, but the common names that are stereochemically most descriptive are (1S,2S)-ephedrine, and (1R,2R)-ephedrine for the d- and l-pseudoephedrine enantiomers, (DSF) and (LSF), respectively. For the ephedrine enantiomers (+ EPH) and (-EPH), (1S,2R)-(+)-ephedrine and (1R,2S)-(-)-ephedrine convey the necessary stereochemical information. The chemical structure of the ephedrine isomers differ by the relative spatial orientations of the functional groups or chromophores associated with the chiral centers. The chromophore responsible for inherent CD activity in the near UV is the substituted aromatic ring (Figure 8). Substituted aromatics typically show multiple $\pi \rightarrow \pi^*$ transitions with absorption maxima in the ultraviolet wavelength range of ~210-280 nm.[32]

Tartaric acid exists in three stereochemical forms: l-tartaric acid, d-tartaric acid, and $meso$-tartaric acid. Technically, the compounds are the 2,3-dihydroxybutanedioic acids. l-Tartaric acid is the most common, a by-product of the wine industry. d-Tartaric acid, although sometimes referred to as unnatural tartaric acid, has been found in nature.[30] The $meso$- form is sometimes described as internally compensated or unresolvable tartaric acid.[30] The primary chromophore associated with the tartrates is the unsaturated C=O of the carboxylic acid groups, which exhibits a weak $n \rightarrow \pi^*$ transition with an absorption maximum near 205 nm.[32]

Copper sulfate, $CuSO_4$ is typically purchased as the dark blue pentahydrate crystal. Upon heating, loss of water of hydration leads to the

$$\begin{array}{c} \text{Ph} \\ \text{HO} \blacktriangleright \text{C} \blacktriangleleft \text{H} \\ \text{H} \blacktriangleright \text{C} \blacktriangleleft \text{CH}_3 \\ \text{NHCH}_3 \end{array}$$

(-)-ephedrine

(1R,2S)

$$\begin{array}{c} \text{Ph} \\ \text{H} \blacktriangleright \text{C} \blacktriangleleft \text{OH} \\ \text{H}_3\text{C} \blacktriangleright \text{C} \blacktriangleleft \text{H} \\ \text{NHCH}_3 \end{array}$$

(+)-ephedrine

(1S,2R)

$$\begin{array}{c} \text{Ph} \\ \text{HO} \blacktriangleright \text{C} \blacktriangleleft \text{H} \\ \text{H} \blacktriangleright \text{C} \blacktriangleleft \text{NHCH}_3 \\ \text{CH}_3 \end{array}$$

d-pseudoephedrine

(1S,2S)

$$\begin{array}{c} \text{Ph} \\ \text{H} \blacktriangleright \text{C} \blacktriangleleft \text{OH} \\ \text{H}_3\text{CHN} \blacktriangleright \text{C} \blacktriangleleft \text{H} \\ \text{CH}_3 \end{array}$$

l-pseudoephedrine

(1R,2R)
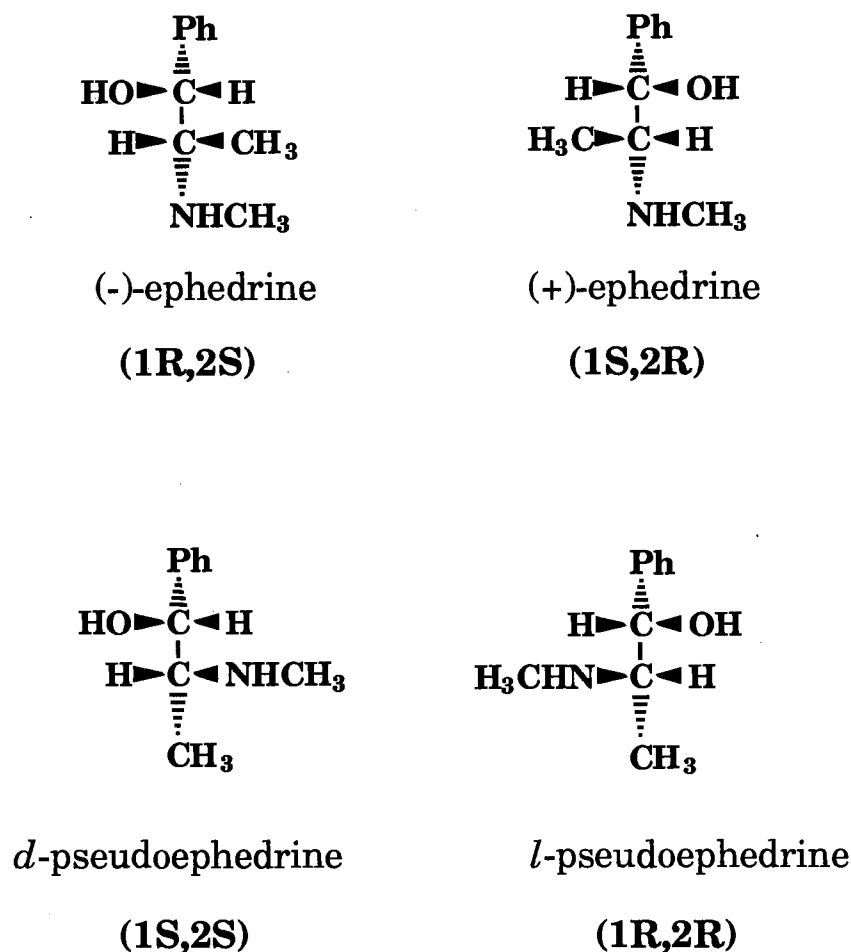
Figure 8. Stereoisomers of ephedrine.

formation of the white anhydrous material. When copper salts undergo dissolution in acidic media, the light blue-green $[Cu(H_2O)_6]^{2+}$ ion is formed. Addition of ligands, i.e. tartrate, leads to the formation of complexes such as the biuret reagent due to displacement of water molecules. The multidentate ligands, such as tartrate, ephedrine, and peptides, form blue copper (II) complexes of considerable stability in basic solution.[33]

<u>Reagents</u>

The modified biuret reagents were prepared using reagent grade $CuSO_4 \cdot 5H_2O$ (Fisher), sodium potassium tartrate (*l*-tartrate; Fisher), potassium hydrogen tartrate (*d*-tartrate; Sigma), and *meso*-tartaric acid (Sigma). Potassium iodide (Baker) was added as an antioxidant.[26] Hydrochlorides of the ephedrine and pseudoephedrine enantiomers of at least 99% chemical purity were obtained from either Sigma or Aldrich Chemical Companies. No information was available concerning enantiomeric purity (EP); each was presumed to be 100% pure and was used as received.

Modified biuret working solutions were prepared by dissolving 3.80 mmole of either *d*-, *l*-, or *meso*-tartrate in ~ 250 mL deionized water in a 500 mL volumetric flask. Then, 5.00 mL of $CuSO_4$ stock solution (0.191 M) and 10.00 mL standardized 5.0 M NaOH solution were pipetted into the volumetric. In addition, 2.5 g of KI was added, and the solution was made up to volume with de-ionized water. Final concentrations of the working solution were 1.91 mM in Cu(II), 7.62 mM in tartrate, and 0.03 M in KI. The final concentration of base was fixed at 0.10 M. At this concentration, the [OH$^-$] is typically in large excess of any added materials and the solution is maintained at a relatively constant pH of ~13.0. The most convenient way of preparing the ephedrine stock working solutions was to dissolve known amounts of the hydrochloride salts in measured volume aliquots of the metal tartrate solution. In this manner, it was possible to prepare test

solutions by adding volume aliquots of working solutions while ensuring that the concentrations of copper ion, tartrate, and base remained constant. Each test solution was prepared by adding the desired volume aliquot(s) of the working ephedrine stock solution(s) into a 25 mL volumetric flask by electronic motorized pipette. The volumetric flask was brought to volume using the modified biuret working stock solution. This ensured that the total $[Cu]^{2+}$ is held constant at 1.91 mM. The copper ion concentration was always kept in excess of the total ephedrine analyte concentration by at least 20%. In addition, to ensure that the stoichiometry for the ligand exchange reaction was 1:1, the tartrate:ephedrine ratio was maintained at $\geq$ 4:1. When binary mixtures were prepared, volume aliquots were added from the stock solutions such that the entire mole fraction range of the ephedrines was represented.

Measurements

All CD spectra were obtained using the Jasco J-500A automatic recording spectropolarimeter previously described. Spectra were generally acquired over the range of 400-700 nm. Instrumental parameters were scan rate of 200 nm/min, acquisitions 2, time constant 0.25, slit width 2 mm, and sensitivity 100 mdeg/cm. The parameters were optimized to provide the minimum acquisition times necessary to produce spectra of sufficient quality. Experiments were carried out under room temperature conditions monitored to $\pm$ 1 C$^{\circ}$.

The modified biuret is a stable analytical reagent.[26] The CD spectra of the parent solution were measured before and after each series of experiments performed on the mixed copper tartrate ephedrine complexes. The average spectrum for the parent was periodically calculated and updated. Under controlled temperature conditions, day-to-day spectral reproducibility for the parent solutions was excellent with a mean value of -246.1 mdeg and a corresponding coefficient of variation of 0.17 for 14 samples measured at 650 nm.

Comparison of Data Analysis Methods

Univariate Approach

The classical implementation of Beer's law is the univariate calibration model. The typical scenario of how spectroscopic data are used for the determination of an unknown consists of the acquisition of a series of absorption measurements vs. concentration. In many instances, data for the entire spectrum are collected and from this a single datum is extracted at the wavelength of maximum absorbance. The additional information contained in the spectrum remains unused. Absorbance data are plotted as a function of concentration to construct a typical Beer's law working curve. Simple linear regression is used to find the statistically best straight line, and corresponding equation, to be used for predicting the concentration of future samples of unknown concentration. Collectively, this calibration/prediction procedure is known as the univariate method.

Multivariate Analysis

The technological basis for the ability to increase the precision in ER determinations is the direct result of the emergence of the laboratory microcomputer for data acquisition and analysis. This has provided the analytical chemist with the ability to accumulate vast amounts of data in a relatively short period of time. It has become much easier to use the additional data to increase the precision and associated predictive capabilities in chemical determinations as commercial software for this purpose has become commonplace. The approach of using more than one measurement (variable or wavelength) per sample (object) for spectrochemical analysis results in what is known as an overdetermined system. Although such a system has no unique solution, systematic methods for data reduction can be employed to reduce the number of variables to match the number of samples.[34] If the number of variables is less than the number of samples, then a solution may not exist due to collinearity.[35]

The statistical techniques that are used for simultaneously extracting quantitative information from many measured variables are collectively referred to as multivariate calibration methods.[36] The multivariate methods most often encountered in the literature are classical least squares (CLS), inverse least squares (ILS), principal component

analysis (PCA), principal component regression (PCR), and partial least squares analysis (PLS1) and (PLS2).[36,37,38]

The linear least squares (LS) method for univariate analysis is one of the oldest and simplest statistical methods for analytical calibration and prediction and is included here as a basis against which to compare the multivariate methods. The LS calibration presumes the existence of a linear relationship between the analyte concentration and the measured response variable. Any errors are assumed to be confined to indeterminant error in the measured y-variable and are further assumed to be normally distributed with zero mean.[39] The resulting calibration line represents the statistical situation such that the residuals, or differences, between the calibration line, and the individual data points are simultaneously minimized.

Classical least squares is the most elementary of the factor analysis methods. It is a multivariate technique and can be thought of as simple linear regression applied to several variables. Although CLS is not typically presented as a factor analysis method, it can be classified as such since the spectral data can be represented in matrix form as the product of two smaller matrices. All of the assumptions of simple linear regression hold for CLS; an additional advantage is an increase in precision over the univariate method as a direct consequence of the use of the additional data points taken from the full spectrum data acquisition.[38] This approach is a very reasonable one for a "well behaved system"; that is, one that is

described by linear responses, no interferences from co-absorbers, low noise, no analyte-analyte interactions, and no collinear responses.[36] A major disadvantage of the method is that all chemical components that absorb in the spectral region of interest must be identified and included as part of the calibration model.[38] Data modeled using CLS use all available variables in order to construct the model used for predictions. Irrelevant information may be difficult to detect, and any such information that is present in the spectral responses, including noise effects, is included in the model.[36] The requirements for LS analysis are fairly rigid, whether in the case of simple linear regression (one independent variable) or general multiple linear regression (many independent variables). Because the requirements concerning the distribution of errors in the y-variable(s) have a serious effect on the construction of a calibration model, outliers and collinearities will have a profound negative effect on the model.

A variation on the CLS method, the inverse least squares method (ILS), offers several advantages over its counterpart. The basis for ILS is, in terms of absorption spectroscopy, the assumption of an inverse relationship such that concentration is a function of absorbance; i.e., an inverse of Beer's Law. There are several desirable outcomes of the inverse Beer's Law approach as it is applied to quantitative spectroscopic analysis:

- Evaluation of the equations provides for an explicit solution for the unknown analyte knowing only the values of the measured absorbances.

- To create a calibration model, the only quantity that need be known is the concentration of the compound of interest; the compounds that are not to be quantified, as well as certain other types of interferences in the mixture, must be present and modeled implicitly during the calibration step.

- It is not necessary to know the values for the molar absorptivities.

ILS is subject to the same problems of collinearity and noise as is CLS. Additionally, as an artifact of the matrix solution for the least squares algorithm, the ILS method is restricted to a smaller number of frequencies than is its CLS counterpart, which may result in the loss of some of the improvements in precision achieved by full spectrum CLS.[38]

Principal component analysis represents an attempt to manage the collinearity problems associated with CLS and ILS while still realizing the benefits of signal averaging offered by full spectrum acquisition in CLS. An additional advantage of PCA lies in its ability to compress the spectral data in such a way as to partition noise and other sources of random error into a secondary group of factors that can be ignored in the construction of the calibration model.[40]

An accepted definition for PCA has been offered by The American Society for Testing and Materials: principle component analysis is "a mathematical procedure for resolving sets of data into orthogonal components whose linear combinations approximate the original data to any desired degree of accuracy. As successive components are calculated, each component accounts for the maximum possible amount of residual variance in the set of data. In spectroscopy, the data are usually spectra,

and the number of components is smaller than or equal to the number of variables or the number of spectra, whichever is less."[41]

A more detailed accounting of the processes involved in PCA follows. The mathematical algorithm referred to in the definition of PCA consists of matrix operations, which, when applied to the original data set, results in the formation of a new coordinate system by which the spectral intensities and component concentrations can be described. The reasoning behind the formation of this new coordinate system can best be explained by analogy to the CLS case. The matrix form of the Beer's law expression for m calibration standards that contain l chemical components with each spectrum containing n digitized instrument responses for the CLS case is

$$\mathbf{A} = \mathbf{CK} + \mathbf{E_A} \tag{25}$$

where $\mathbf{A}$ can be defined as an m x n matrix of calibration spectra, $\mathbf{C}$ can be defined as an m x l matrix of component concentrations, and $\mathbf{K}$ can be defined as an l x n matrix of absorptivity-pathlength products. $\mathbf{E_A}$ is then the m x n matrix of spectral errors not accounted for by the model. The PCA model parallels its CLS counterpart

$$\mathbf{A} = \mathbf{TB} + \mathbf{E_A} \tag{26}$$

where $\mathbf{T}$ is defined as an m x h matrix of intensities in the new coordinate system and $\mathbf{B}$ is a new h x n matrix of full spectrum vectors analogous to the $\mathbf{K}$ matrix in the CLS system.

At this juncture, a few definitions are in order. In the CLS model, the **K** matrix can be thought of as pure component spectra (the rows of **K**), and in the vernacular of chemometrics, these rows would be referred to as factor loadings. Conversely, the elements in the **C** matrix can be thought of as the concentrations associated with the pure component spectra and are referred to as the scores. The difference in the two models can be found by examining the results of the decomposition of the matrix of calibration spectra, **A**, into the product of the two smaller matrices, **T** and **B**. In CLS, the basis vectors are the pure component spectra, while in PCA, these vectors are replaced by the loading vectors resulting from the PCA algorithms. Additionally, the intensities or scores that are the concentrations in CLS are transformed into values in a new coordinate system for which a linear relationship to the original concentrations can be modeled.[38]

The significance of PCA analysis lies in the characteristics of the basis vectors that describe the new coordinate system. The resulting loading vectors have the mathematical property of being orthogonal to each other. If in three-dimensional space two vectors are orthogonal, then the angle separating them will be 90°.[37] It is this extremely useful mathematical property that describes the behavior of a single set of parameters or variables such as the individual loading spectra. The practical significance of orthogonal loading spectra is that they can be evaluated independently of each other. This is the property that allows the

algorithms used in multivariate analysis to deal with the problems of collinearities.

The most commonly used algorithm for PCA is the Nonlinear Iterative Partial Least-Squares algorithm (NIPALS), which was developed by Wold.[42] NIPALS is an iterative algorithm that results in the step-wise extraction of full spectrum loading vectors from the **A** matrix ranked in order of their contribution to the total variance in the calibration spectra. The loading vectors are removed from each calibration spectrum in turn and the process is repeated on the spectral residuals. The process continues until a sufficient number of iterations have been completed to reach the requisite degree of accuracy. This iterative approach ensures that most of the variance is explained by the first few loading vectors, with a substantial amount of the spectral noise being distributed in the remaining vectors. If the end result of the analysis is quantitative, then the PCA can be followed by a regression step.

Principal component analysis followed by regression is termed principal component regression (PCR), and it can be useful for quantitative analysis. Although the loading vectors generated by PCA result in an optimal least squares reduction of errors in the new relative coordinate system, PCA may not generate the optimal ones for concentration prediction.[38] This is a consequence of the manner in which the PCA algorithm generates loading vectors. In order to improve prediction ability, the PCA algorithm was modified to produce loading vectors that take into

account the spectral information in the **A** matrix as well as the information in the component concentrations matrix. This resulting modification to the PCA/PCR algorithm is known as partial least squares analysis or PLS.

Partial least squares analysis is similar to PCA in the manner in which the **A** matrix is decomposed. Both methods employ algorithms that calculate the loading vectors and scores in a stepwise manner until a model with the desired degree of precision and accuracy has been obtained. The PLS algorithm is, to a large extent, the NIPALS algorithm modified to generate concentration dependent loading vectors from the decomposition of the **A** matrix. After the concentration dependent loading vectors, **B**, and the scores, **T**, are calculated, the scores are related to the concentrations or concentration residuals in turn. This results in the generation of loading vectors with the greatest predictive ability early in the iteration process.[38]

Results and Discussion

The CD spectrum for the Cu(II)-*l*-tartrate complex parent solution consists of a broad intense Cotton band of negative sign that maximizes around 650 nm (Figure 9). In the case of the *d*-tartrate isomer, the spectrum would be the mirror image of Figure 9. The *meso-* form has no CD spectrum. The CD activity is a result of the complex formed when the chiral tartrate ligand binds to the copper ion. More specifically, the CD spectrum results from the asymmetric distortions of the ground and excited state ligand field orbitals. An induced CD signal of this magnitude
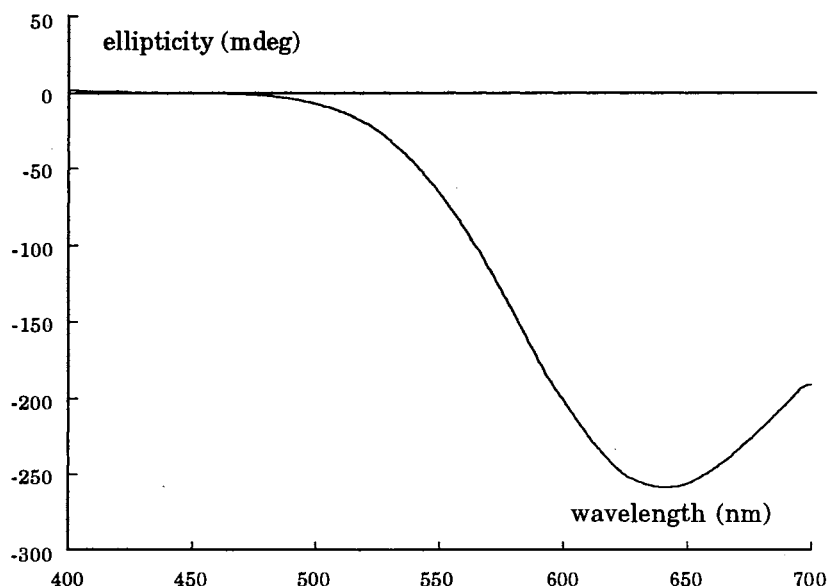
Figure 9. Circular Dichroism spectrum for a 1.91 mM solution of the Cu(II)-*l*-tartrate reagent in aqueous base.

is seldom encountered in the visible region of the spectrum. Even intrinsic CD spectra associated with the aromatic and carbonyl chromophores in the ultraviolet range of 230 to 320 nm are seldom of this magnitude and quality. This is partially due to the fact that the molar absorptivity, $\mathcal{E}$, in the UV for aromatic chromophores are typically very large, while $\mathcal{E}$ for the copper complex is much smaller. The significance of this is that when measurements are taken in the visible region, the CD signal can be measured against a relatively low background absorbance. This provides spectra of exceptional quality and a lower limit of detection by virtue of a much more favorable signal to noise ratio. At a wavelength near 400 nm, there is the beginning of a positive band that can be attributed to the

anomalous dispersion resulting primarily from n–π* transitions in the bound and free tartrate ions.

Cu(II) is a good choice for the host metal ion as it forms very stable complexes.[43] In particular, the stability of 5-membered rings formed between Cu(II) and amino-alcohols is well documented.[44] Additionally, Cu(II) forms complexes that undergo very rapid solvent exchange into the first coordination sphere. Typical solvent exchange rates are on the order of 10^9 sec^{-1}.[45]

Földi et al.[46] have studied the conformational aspects of copper chelates of 2-amino-alcohols. Although their studies did not include the conformational questions of ephedrines in solution, the results are interesting and indirectly support the postulate of the formation of 1:1 mixed complexes or ligand exchange in solution. An argument is presented in favor of the formation of a 4-coordinate 2:1 complex consisting of two 5-membered rings centered about a square planar geometry for the Cu(II) ion. For the ephedrines, oxygen and nitrogen atoms in the OH and NHMe groups would act as the Lewis base donor atoms. Complexes of the racemic ephedrine and pseudoephedrine enantiomers were produced, with the pseudoephedrines being the more stable due to proximal location of the ligand groups. Results showed the copper ephedrine complex to be the less stable of the two, decomposing readily when dissolved in aqueous organic solvents or in alcohols. In either case, the decomposition product was the copper hydroxide precipitate. Furthermore, the more stable

pseudoephedrine complex was insoluble in both ammonia and alkaline tartrate solutions. The postulate was that this is an indication of the difficulty of closure of the ephedrine moiety by chelation into the ring form.[46] This does not disagree with the present observations, as both *l*-pseudoephedrine and mixtures of the *l*- and *d*-enantiomers precipitated when dissolved in the modified biuret reagent at concentrations of 12 and 9 mg/mL respectively. When any one of the isomers is added to the modified biuret reagent under appropriate stoichiometry, a CD spectrum can be recorded that possesses spectral features in addition to those of the spectrum of the modified biuret reagent alone (Figure 10). This implies that solution conditions exist that allow for closure of the 5-membered ring for one ephedrine resulting in the formation of the mixed
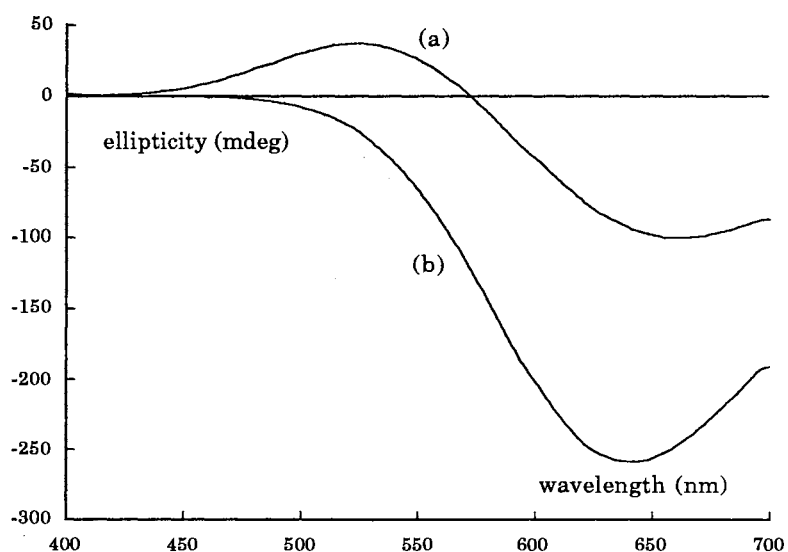
Figure 10. Circular Dichroism spectrum for a) 1.61 mM *d*-pseudoephedrine showing unique spectral features and b) Cu(II)-l-tartrate reagent (similar to Fig. 9, included for comparison).

copper/ephedrine/tartrate complex that is soluble in the modified biuret reagent.

An equation that describes the exchange equilibrium between the bound ligand, such as tartrate, T, and an analyte ligand, such as ephedrine, E, is

$$CuT_x + yE \leftrightarrow CuET_{(x-y)} + yT \tag{27}$$

This is valid under conditions where the host complex is in large enough excess to drive the reaction towards completion and fix the stoichiometry of the ligand exchange at one. Since CD spectropolarimetry is a modified form of absorption spectroscopy, the equation that relates the measured ellipticity to the concentration is:

$$\psi = \left\{ \theta_u b [CuT_x] + \theta_c b CuT_{(x-y)} \right\} \tag{28}$$

where ψ is the measured ellipticity, b is the pathlength, and θ_u and θ_c are the molar ellipticities for the CuT_x and mixed ligand complexes, respectively. An induced CD spectrum is expected for a chiral analyte, even if the tartrate ligand is achiral as in *meso*-tartrate. In this case, the first term on the right contributes nothing to the CD signal and the induced CD signal from the second term is sufficient to determine a chiral analyte.

The induced CD spectra for the mixed complexes of Cu(II) with *meso*-tartrate and each of the four ephedrines are shown in Figure 11. They

Figure 11. Circular Dichroism spectra for the mixed Cu(II) complexes with equimolar solutions of: (a) d-pseudoephedrine, (b) (-)-ephedrine, (c) (+)-ephedrine, and (d) l-pseudoephedrine with *meso*-tartrate.

consist of two distinct mirror image pairs that allow for discrimination between diastereoisomers but not between enantiomers. In contrast, CD spectra for equimolar concentrations of the same uncomplexed isomers measured in the UV consist of two equivalent mirror image pairs and show no unique features for discrimination (Figure 12).

Changes in the spectrum of the copper tartrate complex, which result from the displacement of tartrate ligand by ephedrine to form the mixed complex, can be attributed to several factors that include changes in the inherent chirality of the first coordination sphere, distortions of the out-of-plane ring conformations, and changes due to the effects of through space ligand-ligand interactions. From the unusual distinction of being
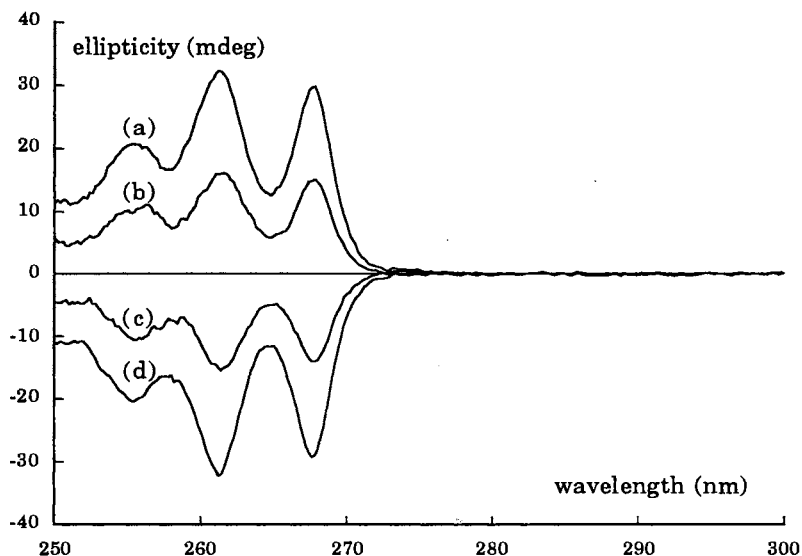
Figure 12. Circular Dichroism spectra for equimolar solutions of the uncomplexed stereoisomers of ephedrine in aqueous acid: (a) (-)-ephedrine, (b) *l*-pseudophedrine, (c) *d*-pseudoephedrine, and (d) (+)-ephedrine.

able to differentiate between diastereoisomers and enantiomers, and in spite of the fact of the inherent achiral nature of *meso*-tartrate, very specific ligand-ligand interactions must exist in these mixed complexes. This implies that there are distinctly different intermolecular bonding associations between the local asymmetric centers on the two adjacent carbons of the tartrate and the opposite stereochemistries offered by the chiral centers on the ephedrine moieties.

When both enantiomers are present, two mixed ligand diastereisomeric complexes are formed. Although these complexes would, in theory, have different formation constants,[29] the actual difference is small compared to the absolute magnitudes of the complexes *per se*. If

conditions are held such that the host complex is in large excess, both enantiomers will be essentially completely complexed as shown by equation (29)

$$CuT_x + \left(\frac{yE}{2} + \frac{yE'}{2} \right) \leftrightarrow CuET_{\left(x - \frac{y}{2} \right)} + CuE'T_{\left(x - \frac{y}{2} \right)} + yT \qquad (29)$$
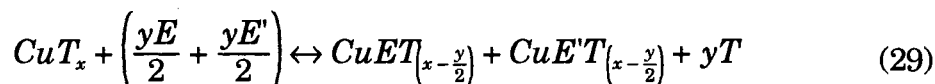
where E and E' represent the enantiomers in a racemate or equimolar mixture of ephedrines. The corresponding Beer's law expression is:

$$\psi = \theta_u b \left[CuT_x \right] + \theta_E b \left[CuET_{x - \frac{y}{2}} \right] + \theta_{E'} b \left[CuE'T_{x - \frac{y}{2}} \right] \qquad (30)$$

In order to discriminate between enantiomers, it is a prerequisite condition that the molar ellipticities for the mixed complexes, θ_E and θ_E', be different for the respective enantiomers. It is evident from equation 30 that enantiomers are indistinguishable when the host ligand is the achiral *meso*-tartrate, since the θ values for the mixed complexes will be equal in magnitude but opposite in sign. In contrast, when the spectra for the mixed ligand complexes with *l*-tartrate (Figure 13) are examined, each spectrum is unique, there are no mirror images, and all are reduced in magnitude as compared to the copper-*l*-tartrate host spectrum. As a result, the necessary condition of unequal molar ellipticities is satisfied in every case. The specific chiral-chiral interactions that result in an induced CD signal can be predicted from equation 30, which would suggest that the ultimate degree of analytical selectivity is determined by the molar ellipticity values
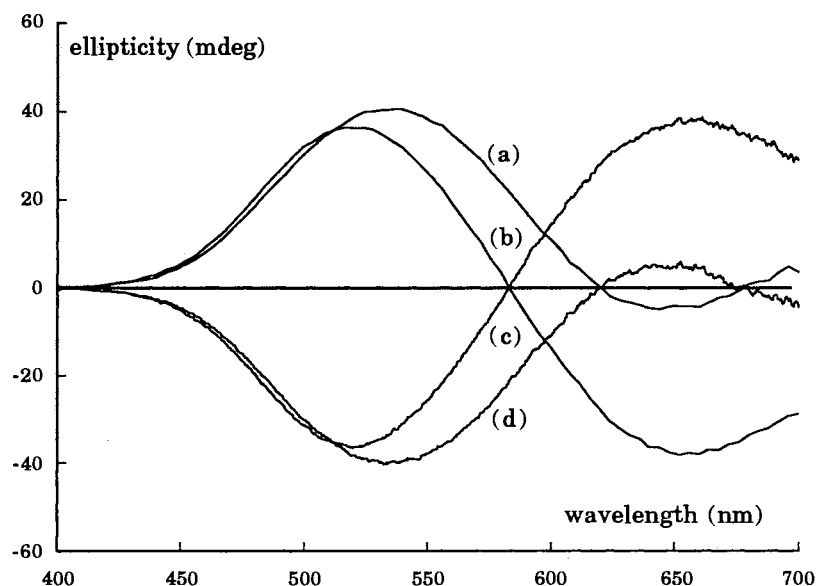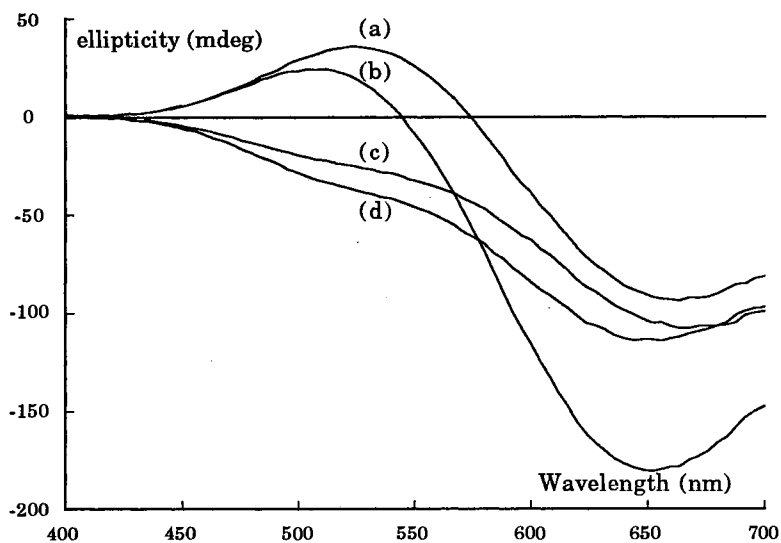
Figure 13. Circular Dichroism spectra for the mixed Cu(II)-complexes with equimolar solutions of: (a) d-pseudoephedrine, (b) (-)-ephedrine, (c) l-pseudoephedrine, and (d) (+)-ephedrine with l-tartrate.

for the mixed ligand complexes. Spectra for (DSF) and (LSF) and for (-)EPH and (+)EPH are shown as a function of analyte concentration in Figure 14 and Figure 15, respectively.

Comparisons among the spectra show a sign inversion at higher concentration for the diastereoisomers d-pseudoephedrine and (-)-ephedrine, but not when the analyte is l-pseudoephedrine or (+)-ephedrine. Curves for the last two isomers do, however, intersect with the spectrum for the host copper tartrate complex at characteristic isosbestic points that are separated by about 10 nm. Isosbestic points are relatively rare in the CD literature.[47,48] In common UV-visible spectroscopy, they are usually associated with some type of acid-base or metal-complex formation equilibrium.[49] An isosbestic point is evidence for an equilibrium between
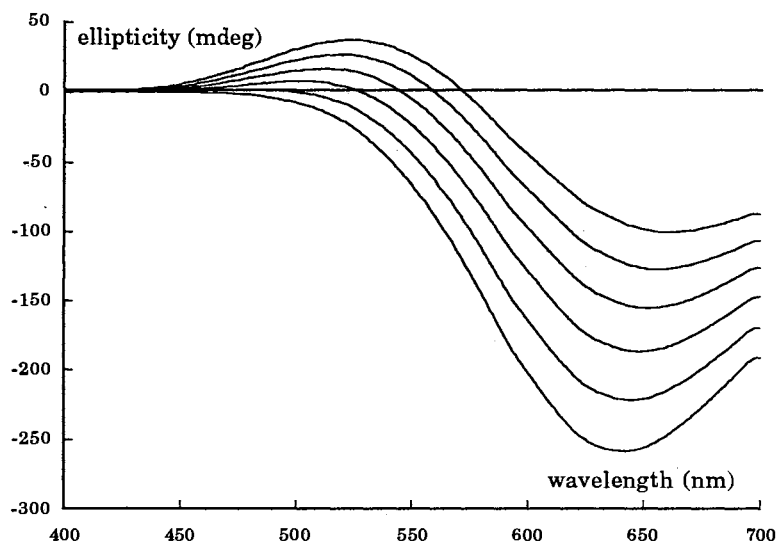
Figure 14a. Circular Dichroism spectra vs. solution concentration for the mixed Cu(II)-complexes with d-pseudoephedrine.
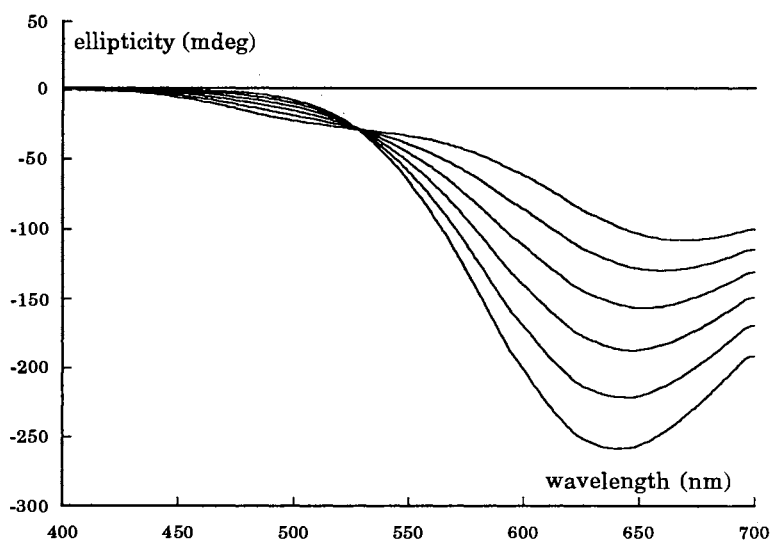
Figure 14b. Circular Dichroism spectra vs. solution concentration for the mixed Cu(II)-complexes with l-pseudoephedrine. The isosbestic point is located at 527 nm with an ellipicity value of -24.9 mdeg.
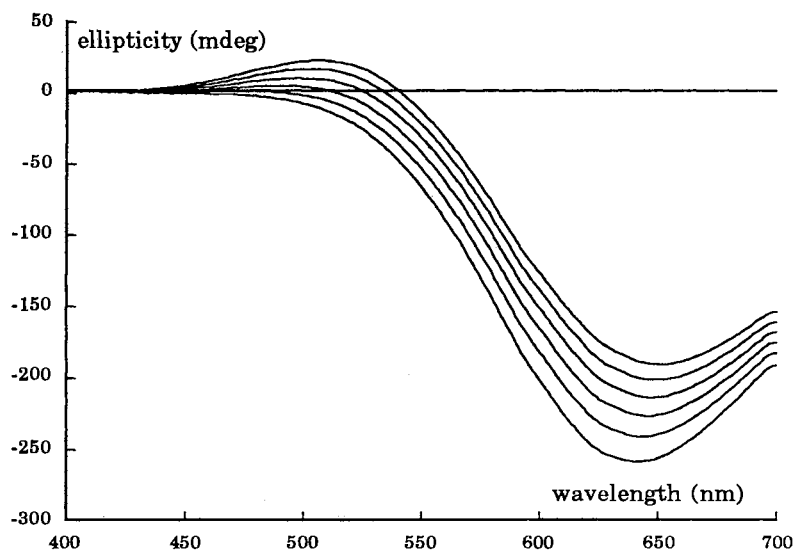
Figure 15a. Circular Dichroism spectra vs. solution concentration for the mixed Cu(II)-complexes with (-)-ephedrine.
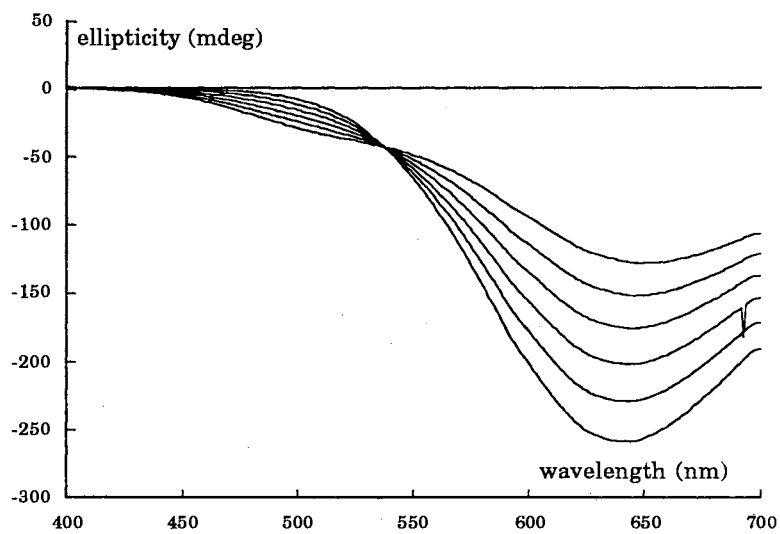
Figure 15b. Circular Dichroism spectra vs. solution concentration for the mixed Cu(II)-complexes with (+)-ephedrine. The isosbestic point is located at 538 nm with an ellipicity value of -43.7 mdeg.

two absorbing species that have the same molar absorptivity at a common wavelength. The existence of an isosbestic point is one criterion that is used when characterizing an interconvertable binary system.[50] In terms of this study, the isosbestic point is also evidence for the existence of two metal complexes over the chosen concentration range that have a common molar ellipticity at the isosbestic wavelength. The phenomenon of an isosbestic point should be quite general for any chiral ligand that might replace tartrate in the host complex, since the spectrum for only one member of an enantiomeric pair can intersect with the host complex spectrum.

When the host complex is formed with d-tartrate, a similar situation is observed, but instead of the isosbestic point being associated with the l-pseudoephedrine or (+)-ephedrine diastereoisomers, it occurs with the other member of the diastereoisomeric pairs. The existence of the isosbestic point is analytically significant because it allows for the construction of a linear calibration curve at this wavelength and is the basis for the univariate method.

As a result of the unique spectral features associated with the mixed complexes, in particular the isosbestic point, any mixture of isomers will have a net, non-zero spectrum, including racemates. These conditions form the basis for the application of univariate methods to data analysis. The Beer's law expression for this situation can be described by an equation similar to (30) for the racemic modification except that $[E] \neq [E'] \neq y/2$. Since the typical calculation for an EP involves the simultaneous solution of a set

of linear equations, generated from two independent experiments, the present situation is uncommon in the sense that it can potentially allow for a reduction in the number of experiments that are needed to make the calculation from two to one. Although it should be possible to calculate the enantiomeric ratio from a set of linear equations based on measured molar ellipticities of the pure components in solvents of different chirality, the presence of isosbestic points renders this approach unnecessary.

At the isosbestic point in a mixture of enantiomers with Copper-*l*-tartrate, the signal will be non-zero and directly proportional to the concentration of the only isomer whose spectrum does not intersect with the spectrum of the host copper tartrate complex. Construction of a working calibration curve for the determination of [DSF] in a DSF:LSF mixture begins by measuring the signal intensity for the mixture at the isosbestic wavelength. This value is corrected for the value at the isosbestic point for the copper *l*-tartrate parent solution and plotted as a function of [DSF]. Data normalized in this manner produces a linear plot over a concentration range spanning two orders of magnitude with a near zero intercept. The calibration curve, shown as spectrum (a) in Figure 16, prepared from a series of copper *l*-tartrate solutions of *d*- and *l*-pseudoephedrine mixtures, whose concentrations span the whole range of mole fractions, shows good linear correlation with the concentration of the *d*-enantiomer.
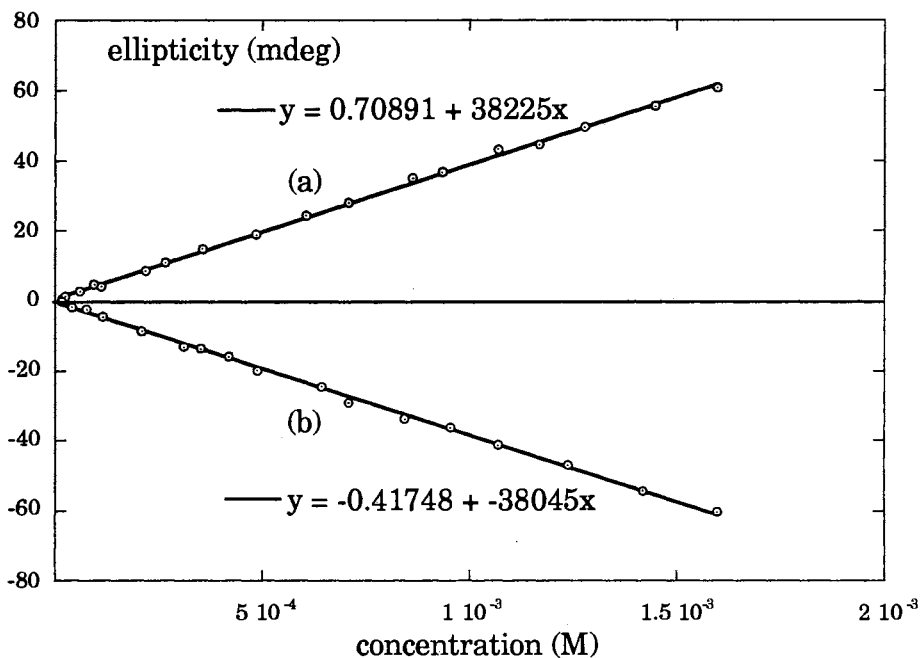
Figure 16. Correlation curves for ellipticities measured at the isosbestic points vs. (a) [DSF] for a series of DSF and LSF mixtures with Cu-*l*-tartrate and (b) [LSF] for a series of DSF and LSF mixtures with Cu-*d*-tartrate. The DSF and LSF mixtures are of variable ratios and total concentrations.

In order to calculate an EP or isomeric purity (IP) using the concentration of the *d*-enantiomer obtained from the isosbestic measurement, additional information must be obtained in the form of the total analyte concentration. This could be accomplished by the independent measurement of either the total analyte concentration or of the concentration of the other enantiomer that, when added to the first enantiomer concentration, will give the total analyte concentration. In either case, it is desirable to avoid the use of a non-selective detector that would negate the advantages of selectivity offered by the CD detector.

The univariate method for determining the total analyte

concentration that retains the analytical advantages afforded by the CD

detector relies on the behavior of the system when a fixed amount of

ephedrine is added to the copper tartrate host. As can be seen in Figure 17,

a reduction in the absolute magnitude of the copper tartrate parent solution

occurs upon the addition of a fixed amount of either the DSF or LSF stock

solution. This constant difference is observed at all ratios and over a wide
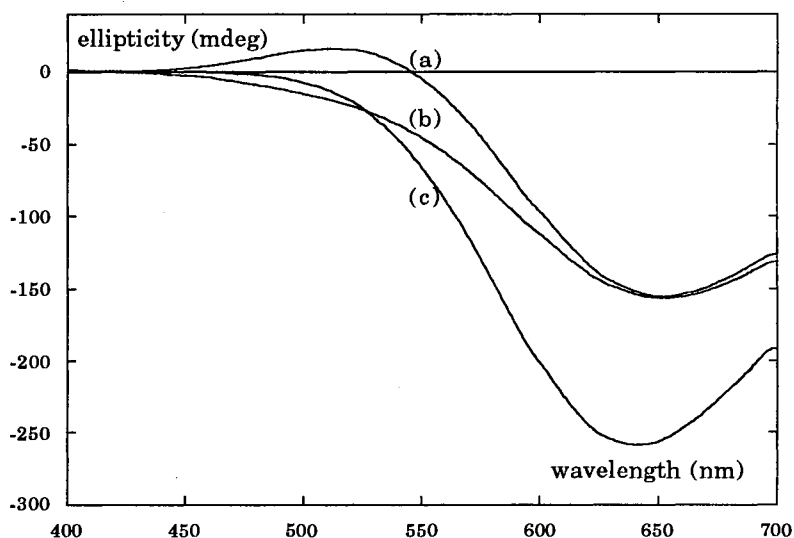
Figure 17. Circular Dichroism spectra for addition of equimolar
concentrations of (a) d-pseudoephedrine and (b) l-pseudoephedrine when
added to (c) the Cu-l-tartrate host. A near constant difference from the host
is observed near the long wavelength maximum.

concentration range, making a calibration curve for the total ephedrine

concentration possible. The plot, of total ephedrine concentration vs

measured ellipticity (Figure 18), reveals that the relationship is not a linear

one. This method is referred to as the univariate method for calculation of enantiomeric purities using calculated totals.
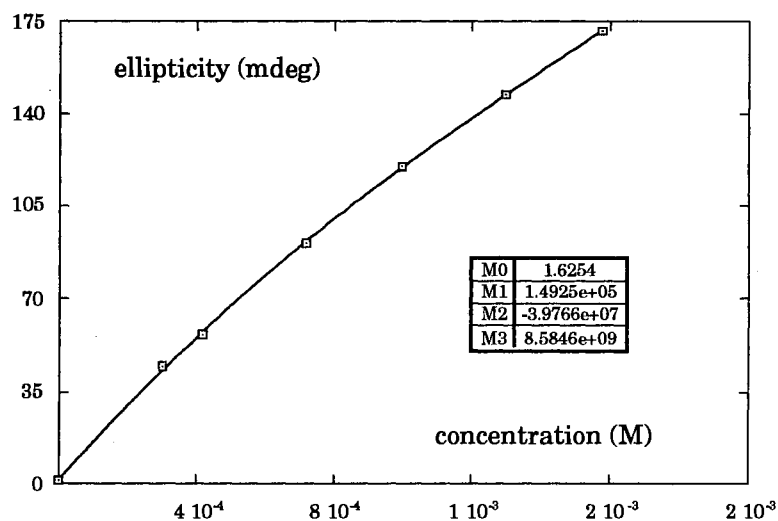
Figure 18. Polynomial correlation curve for ellipticities measured at 630 nm for fixed amounts of ephedrine added to Cu-*l*-tartrate. The coefficients M0 through M3 refer to the coefficients in the polynomial expression.

The second method requires independent measurement of the other enantiomer leading to a calculation of enantiomeric purities using summed totals of enantiomers. This method is based on a repeat measurement made at the isosbestic point for the same isomer mixtures added to the Cu(II)-*d*-tartrate host. This results in a working curve as illustrated in Figure 16b. One disadvantage to this approach is the need for two individual experiments to calculate the ER.

Univariate Results

Results of EP calculations based on direct measurement of the d-enantiomer at the isosbestic point and the total based on calibration at 630 nm are shown in Table I. Total pseudoephedrine concentrations were calculated by finding the root of the polynomial expression whose coefficients are shown in Figure 18 at a given measured ellipticity by numeric approximation.[51] Results are less than satisfactory in the critical range of x>0.95. In addition, there is a noticeable positive bias. Since the plot was not optimized in terms of the number of experimental points to be plotted or the degree of the polynomial, it is difficult to account for the exact source of the bias.[52] In light of the difficulties associated with accounting for the random spurious fluctuations in the data, as they pertain to construction of a viable working curve for calculation of the total ephedrine concentration, this approach was abandoned in favor of those to follow.

Table I. Calculated Enantiomeric Purities of Prepared Binary Mixtures Using Univariate Calibration With Calculated Totals[a]

composition	0.990 : 0.010	0.950 : 0.050	0.900 : 0.100
mean (N=3)	1.00 : 0.00	0.956 : 0.044	0.899 : 0.101
C.I. ±	0.004	0.005	0.005

[a] d-pseudoephedrine : l-pseudoephedrine (with l-tartrate)

The univariate method for determining ER that uses total pseudoephedrine concentrations arrived at by summation of the two independently measured enantiomers gives very good predictions for a series of prepared mixtures of pseudoephedrines of anonymous concentration and ER provided that mixtures lie in the mole fraction range $x \leq 0.95$ (Table II). The individual isomer concentrations were calculated using the linear curve fits from Figure 16. Their sums, compared with the prepared total concentrations, have an average positive bias of ~2%. Results are of comparable quality to those from chromatographic methods.[24]

Table II. Calculated Enantiomeric Purities of Prepared Binary Mixtures Using Univariate Calibration With Summed Totals[a]

composition	0.990:0.010	0.950:0.050	0.900:0.100	0.750:0.250	0.500:0.500
mean (N=3)	0.995:0.005	0.945:0.055	0.900:0.100	0.748:0.252	0.500:0.500
C.I.±	0.006	0.004	0.018	0.006	0.009

[a] d-pseudoephedrine : l-pseudoephedrine (with l-tartrate)

Results from the univariate experiment are indicative of the challenge associated with the determination of the ER for a binary mixture in the mole fraction range of 0.95-1.00. This is not necessarily a situation that is unique to ER determinations performed on unseparated bulk samples, but rather it is a more general problem associated with the measurement of the enantiomer that is the minor component and is independent of the detector and/or procedure. Difficulties associated with

the general determination of ER as applied to chromatographically separated samples is offered by Armstrong *et al.* in a review of the nature of errors in ER determinations using chiroptical chromatographic methods.[24] It is evident that an approach to the data analysis must be taken that will allow for an increase in precision, especially whenever one component is in large excess.

PLS2 Multivariate Results

The origin of PLS regression dates back to the 1960s when Herman Wold developed the basic algorithms for modelling and prediction.[53] Since its inception, the method has been applied to several areas of chemistry including, but not limited to, organic, medical, environmental, and analytical chemistry.[54] Of the applications of PLS to analytical chemistry, the larger number use near infrared (NIR) spectroscopy or infrared (IR) spectroscopic data.[55,56,57,58] These regions of the EM spectrum, particularly the IR, are well suited to factor analysis methods because they contain a wealth of spectral information that can be used for calibration and prediction.[38] Although, in general, the amount of spectral information decreases as the wavelength decreases, absorbance by species in the visible spectrum should still produce good models with PLS analysis as a consequence of the spectral information resulting from the overlap of multiple absorption bands.

Multivariate analysis has been used with absorption spectrophotometry in the visible region for the determination of metal chelates. PLS was successfully applied to the analysis of trace metals in multicomponent mixtures by employing a color complexation reaction using dithiooxamide as the ligand.[59] Although the determination of enantiomers using chelation chemistry is similar to the above experiment, it is evident that the choice of ligand chirality and detector are critical to the success of the multivariate method.

For the PLS analysis, three binary systems were prepared using mixtures of the following isomers: DSF/LSF, DSF/ (+)EPH, and DSF/(-)EPH. The rationale of these particular choices for the latter two binary mixtures involves the stereochemical consequences resulting from single inversion of the individual chiral centers of *d*-pseudoephedrine. Determination of the IP of *d*-pseudoephedrine is representative of quality control type problems that are of importance in the pharmaceutical industry. For instance, in the synthesis of a chiral drug, its enantiomer could be formed, which is considered to be an optical impurity. During long-term storage, inversion of configuration is possible leading to the formation of a racemate or an isomeric mixture. For chiral molecules such as *d*-pseudoephedrine, with adjacent chiral centers, inversion could produce either the (+)- or (-)-*ephedrine* diastereoisomer or both, depending upon which of the two side-chain chiral centers are involved (Figures 19 & 20). These processes,
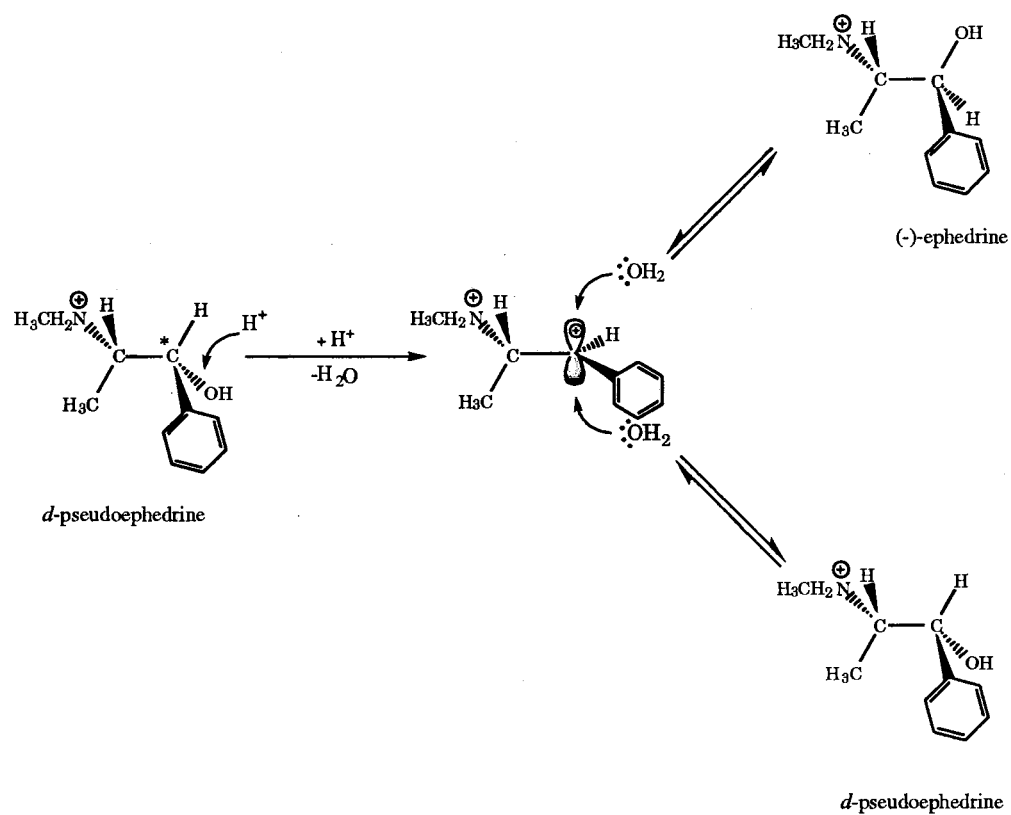
Figure 19. Proposed mechanism for chiral inversion at center #1*.
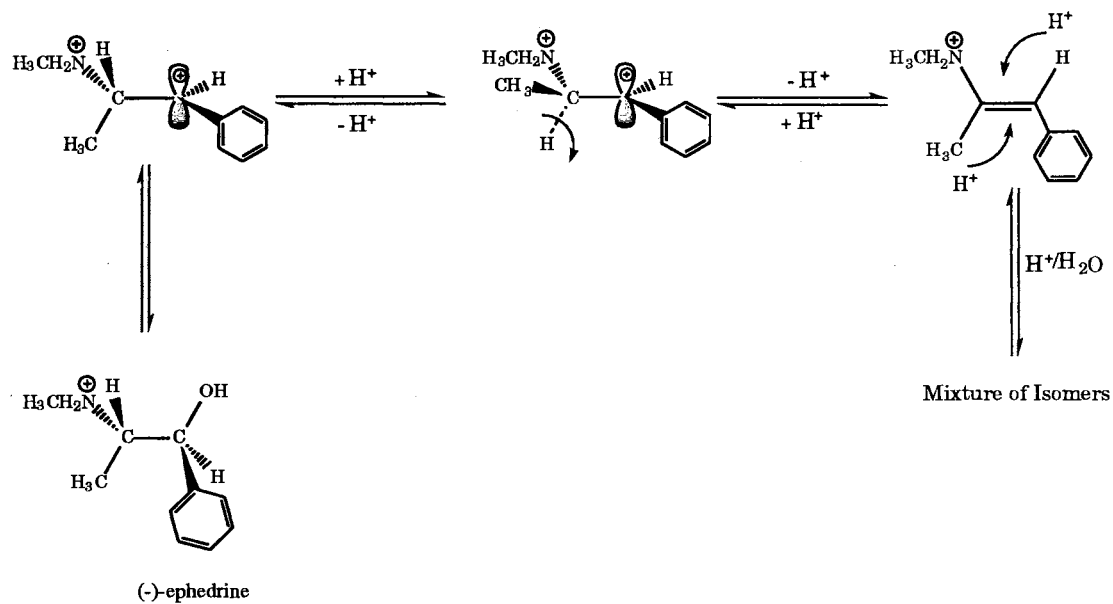
Figure 20. Proposed elimination from carbocation intermediate in Fig. 19.

over the normal shelf life of a product, probably do not happen to any great extent, in which case the most significant mole fraction range is x > 0.95.

For the ephedrine/mixed complexes study, PLS2 analyses were performed using the CD data sets that were collected over the wavelength range 400-700 nm. Data sets were truncated, depending on the binary system used, to correct for the long baseline lead-in that was devoid of spectral information.

Calibration models were prepared using the PLS2 algorithm that is part of the commercial chemometric analysis software package marketed under the name UNSCRAMBLER II (CAMO A/S, Trondheim, Norway).[60] Although the PLS algorithm can be used for analysis and prediction of one component at a time (PLS1), a more general form of the algorithm can be used (PLS2) for simultaneous determination of multiple component concentrations. Although there is empirical evidence for using multiple stepwise PLS1 analyses for multicomponent determinations in lieu of a single PLS2 step[38] for the ephedrine determinations, PLS2 gave similar results while requiring only a single calibration model. PLS2 can give better prediction ability than multiple PLS1 analysis in the case where several strongly intercorrelated Y-variables exist, although this is not the norm. Multiple PLS1 modeling for each y-variable is still preferred for situations where the major calibration errors are the result of non-linearities as opposed to random noise. This is a result of the ability of PLS methods to model certain types of non-linearities in the data. In the case of PLS2,

modeling of these non-linearities can result in a suboptimal calibration model.[37] The fact that in this study the PLS2 performance was on par with PSL1 analysis suggests that random noise, rather than nonlinearities in the data, was the mitigating factor in the determination.

As the basis for the calibration model for each pair of isomers, training sets were prepared using from 18 to 35 binary mixtures which were prepared to cover the entire mole fraction range $x = 0$ to 1. Modelling was done on a maximum of 76 equally spaced data points; the truncated models used fewer numbers of points. Data pretreatment consisted of centering the data about the mean and applying default weights of 1.0 as allowed for in the UNSCRAMBLER program. Mean centering involves subtraction of the average of the calibration spectra from each spectrum; the associated concentration matrix is treated in the same manner. This eliminates the need for the model to fit a nonzero intercept.[38] Since the units in the respective spectral and concentration matrices were constant, and there were no criteria for assigning *a priori* significance to any particular variables, no scaling factor was employed.[35,38] Models were validated by internal cross validation using random segment selection. The optimum fit was afforded by use of the first two principal components and resulted in models that were able to explain greater than 99.8% of the variance in the data sets.

The corresponding calibration model for each pair was used to predict mole fraction compositions for anonymous mixtures. The protocol

followed for calibration of IPs was to calculate the concentrations for both isomers directly so that the model could be validated by comparing the sum of the enantiomer concentrations with the total analyte concentration used to prepare the unknown solutions. There was no bias, and deviations between prepared and calculated total concentrations were within 0.1%. Predicted IP values expressed as mole fractions are given in Table III, together with the imprecisions calculated as confidence intervals (CI). The result is that an overall improvement is seen over the figures obtained using the univariate model, especially in the critical range of x > 0.95.

Table III. Predicted Enantiomeric Purities of Prepared Binary Mixtures Using PLS2 Multivariate Regression Analysis[a,b,c,d]

composition	0.990:0.010	0.950:0.050	0.900:0.100	0.500:0.500	0.100:0.900	0.050:0.950	0.010:0.990
mean (N=3)	0.992:0.008	0.952:0.048	0.905:0.095	0.505:0.495	0.099:0.901	0.047:0.953	0.007:0.993
C.I. ±	0.006	0.019	0.014	0.010	0.005	0.021	0.001

[a] d-pseudoephedrine:l-pseudoephedrine (with l-tartrate)

composition	0.990:0.010	0.950:0.050	0.900:0.100	0.500:0.500	0.100:0.900	0.050:0.950	0.010:0.990
mean (N=3)	0.989:0.011	0.953:0.047	0.904:0.096	0.498:0.502	0.102:0.898	0.055:0.945	0.018:0.982
C.I. ±	0.011	0.005	0.007	0.006	0.009	0.004	0.002

[b] d-pseudoephedrine:(+)-ephedrine (with l-tartrate)

Table III. Continued

composition	0.990:0.010	0.950:0.050	0.900:0.100	0.500:0.500	0.100:0.900	0.050:0.950	0.010:0.990
mean (N=3)	0.958:0.042	0.918:0.082	0.927:0.073	0.477:0.523	0.064:0.936	0.044:0.956	0.033:0.967
C.I. ±	0.020	0.012	0.126	0.030	0.018	0.013	0.032

c d-pseudoephedrine:(-)-ephedrine (with l-tartrate)

composition	0.990:0.010	0.950:0.050	0.900:0.100	0.500:0.500	0.100:0.900	0.050:0.950	0.010:0.990
mean (N=3)	0.992:0.008	0.950:0.050	0.900:0.100	0.503:0.497	0.108:0.892	0.055:0.945	0.013:0.987
C.I. ±	0.012	0.006	0.011	0.003	0.014	0.011	0.019

d d-pseudoephedrine:(-)-ephedrine (with $meso$-tartrate)

The chemistry is not constrained by either the univariate or the multivariate models by requiring that the total analyte concentration be fixed at a particular single value for every determination. However, the total ephedrine concentrations were maintained at values that were never allowed to exceed the Cu(II) ion concentration in the reagent. The only overriding constraint is that the analytical reagent concentration must be in large excess over the total analyte concentration. The experimental conditions are such that they make application of the method fairly general. Absorption by the reagent is not excessive at the concentration used in this series of experiments, and higher concentrations could be used if necessary to ensure that the tartrate to analyte ratio is, in fact, greater than 4:1 without adversely affecting the signal to noise ratio. The analytically

determining factor is the magnitude of the spectral change that accompanies the ligand exchange. Changes will be minimized if [CuL$_2$] is too high compared to the concentration of the substituting ligand. Because of the inherent intensity of the CD signal of the modified biuret reagent, the relative change in the spectrum can be optimized by diluting the reagent, which can, in effect, result in lower analytical sensitivities. For each potential new chiral analyte, the concentration of the reagent should be optimized.

The greatest imprecisions were expected for IP measurements for binary mixtures of d-pseudoephedrine and (-)-ephedrine (Table III) because the spectra of their mixed ligand complexes with l-tartrate are the most similar (Figure 21). In spite of this, IPs are still quite acceptable when compared with the results from other methods. Mixtures of these diastereoisomers were also analyzed using the Cu(II)-$meso$-tartrate reagent. Results from these determinations are much improved over those from the reagent based on the l-tartrate exchange reaction, which is an indication of the ability of the $meso$- form to discriminate between diastereoisomers (Table III).

Calibration models for the binary mixtures are distinct and are not interchangeable. This could provide useful information for confirming the identity of the potential inversion product(s) or other optically active products that might result from inversion of d-pseudoephedrine in solution. Additional qualitative information could be provided by measuring spectra
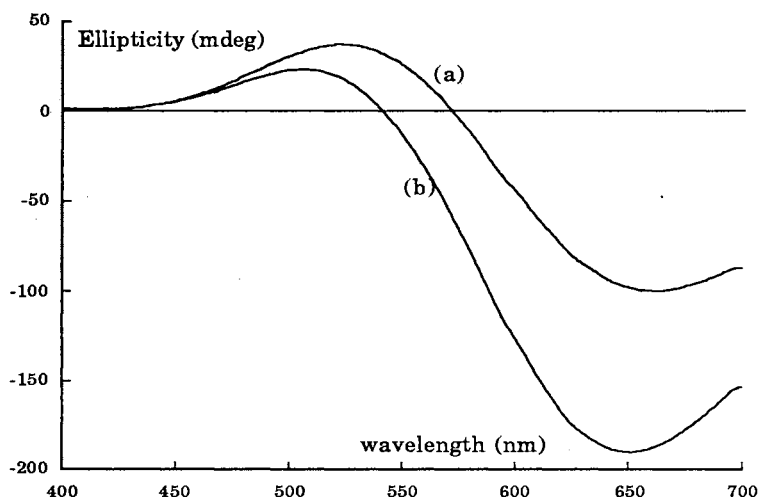
Figure 21. CD spectra for the mixed Cu(II) complexes of equimolar solutions of (a) *d*-pseudoephedrine and (b) (+)-ephedrine with Cu-*l*-tartrate.

for binary mixtures with both the *l*- and *meso*-tartrate reagents and comparing these spectra with the unknown. The *l*-tartrate can give discriminatory information concerning enantiomers, while the *meso*-tartrate reagent can provide information about diastereoisomers.

The performance of the method in its present state of development has not been tested in the presence of chemical impurities. Achiral impurities that do not displace tartrate would be expected to have little effect on the model. Changes in the spectrum due to displacement of tartrate with other chirals would likely make predictions based on the current models suspect, at best, but such impurities could be implicitly modeled during the calibration phase as necessary. Perhaps the most serious threat to the model would be an achiral impurity that might displace tartrate. An achiral ligand such as creatinine[1] would cause the spectrum to decrease in

intensity while leaving the basic features of the CD spectrum intact, and it would be difficult to account for in the model.

The method of a chiral ligand exchange reaction followed by PLS analysis could be applied immediately to the measurement of IPs in bulk drugs or standard reference materials, while it could be applied to commercial drug formulations with a minimum of further development. With some adaptation, the reagent could be introduced through a post-column reactor in conventional column HPLC. Future work in the area of the mixed ephedrine complexes should be directed towards determination of the potential inversion product(s) of d-pseudoephedrine in solution. Additional experimentation needs to be done to test the ability of the PLS method to produce viable calibration models for the prediction of IPs in the presence of potential interferences from achiral and chiral ligands.

CHAPTER V

USE OF INDUCED CIRCULAR DICHROISM TO FACILITATE THE STUDY OF MOLECULAR ASSOCIATION REACTIONS IN AQUEOUS SOLUTION BETWEEN CELLO-OLIGOSACCHARIDES AND RELATED SACCHARIDES WITH POLY-AROMATIC DYES

Introduction

Cellulose is a naturally occurring polysaccharide composed of a series of glucose units linked by a β-1,4-glycosidic type bond.[61] It is primarily a structural polymer, usually found as a component of higher plants, but it also occurs in the cell walls of certain microorganisms and the outer surfaces of some animal cells.[62] The structure of the cellobiose dimer repeat unit is shown in Figure 22 as an illustration of the β-1,4 linkage.[30] The β linkages result in chains of D-glucose units that ultimately form insoluble fibrils.[62]
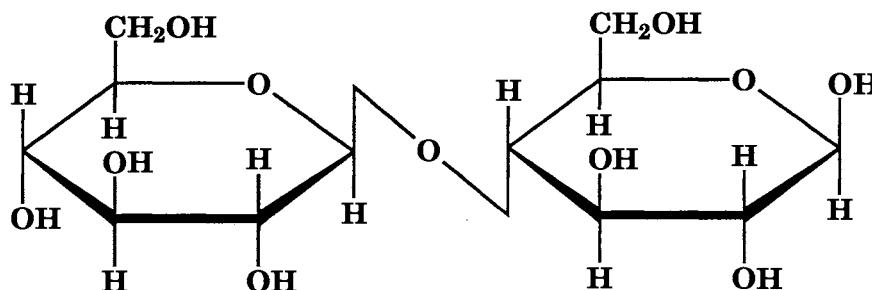
Figure 22. Cellobiose dimer illustrating the β-1,4 linkage of anhydroglucose units.

Amylose (starch) is also a naturally occurring polysaccharide, but its function is typically food storage.[62] The linkage in amylose, by contrast, is an α-1,4 (Figure 23), which results in substantial structural differences from cellulose.[30] As a consequence of these α-1,4 linkages in amylose, the main chains of the polymer assume a helical or coiled conformation. This geometry about the glycosidic bond results in the formation, on a cellular scale, of dense granules.

CH$_2$OH   CH$_2$OH

H   O   H   H   O   OH

H   H

OH   H

OH   OH   H

H   OH   O   H   OH
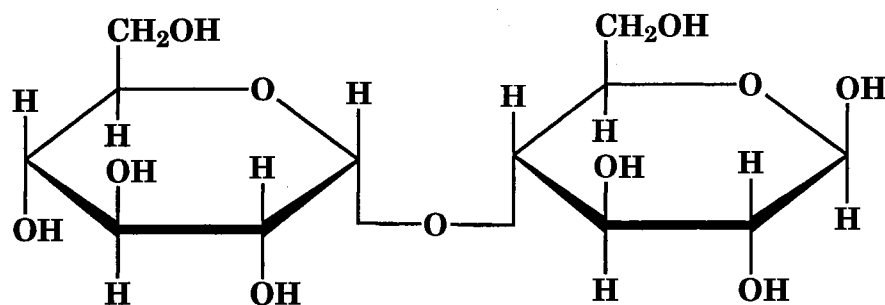
Figure 23. Maltobiose dimer illustrating the α-1,4 linkage of anhydroglucose units.

Like other macromolecules of biological origin, celluloses and modified celluloses are optically active and many are CD active, usually in the UV and far UV. In spite of the inherent difficulties associated with making CD measurements in the far UV, much work has been done in accumulating CD data that have been used to interpret the secondary and tertiary structures of these macromolecules in aqueous solution.[48,63] As an alternative to measuring the inherent CD, it may be useful to exploit certain substitution or molecular complexation reactions to induce a chromophore that absorbs in the visible region into molecules that have no native CD

activity there. In the case of carbohydrates, for example, CD spectra that result from exciton coupling between aromatic substitiuents have been used to interpret the anomeric forms of linkages and the local stereochemistry between neighboring diols in monomeric repeat units.[64,65] Complexations of iodine and 1-butanol with amylose[66] are examples of molecular association reactions. Of the two categories of reactions just mentioned, the molecular association reactions are the most common, especially those that are able to fit into the hydrophobic chiral cavities of the cyclodextrin oligomers.[67]

There is considerable industrial interest in cellulose and derivatives of cellulose.[68,69] In textiles, the interaction of dyes with polysaccharides is of particular interest,[69] while cellulose esters are extremely important to the coatings industries. In terms of basic research, fundamental unresolved problems remain regarding the biosynthesis or formation of higher order crystalline structures of cellulose.[70,71] In addition, there is biochemical interest in the mechanisms of the enzymatic degradation of cellulose.[72,73,74] The objective of this study was to investigate dye-cellulose interactions in solution. Evidence was obtained that gives support for a binding process that involves a hydrophobic mechanism, which is in agreement with previous results from molecular association experiments using cyclodextrin molecules and proteins. This evidence also provides a possible explanation for the binding of the various cellohydrolases to cellulose oligomers.

One of the outcomes of binding an achiral chromophore, i.e. a dye molecule, to an inherently optically active substrate, such as a cello-oligomer, is that the complex that forms exhibits CD activity in the easily accessible visible range of the spectrum. Structural information can be gleaned from the resulting CD spectrum that can yield valuable information about the structure of the chiral host molecule in solution. In this manner, the information can be interpreted in a way analogous to the exciton coupling models mentioned earlier. Complexation with a dye that absorbs in the visible allows for the structural information to be obtained in a manner that avoids the interferences and technical problems associated with far UV measurements.

The crystalline solid synthesized by plants and bacteria is called cellulose I.[61] The bacterium *Acetobactor xylinum* produces, for example, a pellicle, or thin sheet of high purity cellulose I, which is an excellent model compound for investigations concerning the biosynthesis and morphology of cellulose fibrils.[75] Cellulose I appears to be thermodynamically unstable and forms Cellulose II in an irreversible process whenever it is mercerized or regenerated from solution.[61] In 1980, Haigler, Brown, and Benziman reported additional evidence concerning the morphology and stability of cellulose I. They observed that *A. xylinum*, when grown in the presence of the water-soluble fluorescent dye Calcofluor White ST, Table IV, produced a pellicle of cellulose that showed no detectable crystallinity.[76] This was interpreted as evidence that the crystalline structure of cellulose produced

Table IV. Molecular Structures for Active Dyes

Dye name	Structure
Calcofluor	
Congo Red	
Direct Orange #8	
Direct Yellow #1	
Direct Violet #1	
Trypan Blue	
Titan Yellow	

by *A. xylinum* in the absence of the dye arises from a cell-directed coordination of synthesizing sites. A subsequent study revealed a similar effect on cellulose synthesis when Calcofluor was added to the growth medium containing the green algae *Oocystis solitaria*.[77] Haigler has reported a series of water-soluble dyes, whose structures are shown in Table IV, that are effective in modifying the crystalline nature of cellulose produced by *A. xylinum* to varying degrees. Dyes of different structural types that are apparently not effective in modifying the crystallinity of *A. xylinum* cellulose are listed in Table V. Of these, Nile Blue A and Light Green SF Yellowish were reported as inactive by Haigler.

X-Ray[78,79,80] and solid-state ^{13}C NMR[81] structural analyses have been performed on Calcofluor-modified bacterial cellulose. Results from these studies are ambiguous, with X-ray lines attributed to cellulose by one author, while other authors make the assignment to incorporated dye aggregates.[82] Research continues in an effort to understand the factors that affect the formation of the higher-order structures of cellulose. Specifically, the study of chemically altered bacterial and algal celluloses is an ongoing effort to try to determine the relationship between the various biological and physical factors that affect the formation of the higher-order celluloses.[83]

The work discussed above has dealt with the interactions of specific dyes (i.e., Calcofluor and Congo Red) with crystalline forms of cellulose. One question that required further attention was whether or not the dye-cellulose interactions are specific to the bulk insoluble cellulose, or if

Table V. Molecular Structures for Inactive Dyes

Dye name	Structure
Nile Blue A	
Light Green SF Yellowish	
Ethyl Red	
2,6-Dichloroindophenol	
Anthroquinone Blue	
3,3'-Diethyloxadicarbocyanine Iodide	
Acridine Orange	

they would also occur with the soluble oligomeric celluloses in aqueous solutions. Wood[84] conducted preliminary studies of direct dye-saccharide interactions using certain oligo- and polysaccharides. He reported that small shifts in the absorption spectrum of the dye occurred in the presence of the saccharides, but stated that "cello-oligosaccharides showed little or no interaction."[69]

Although proteins, polynucleotides, and carbohydrates are intrinsically CD active, the chromophores absorb in the UV. Carbohydrates are particularly difficult to study as their CD spectra lie in the far UV.[48,63] Ritcey and Gray investigated the interactions between methylcellulose, oligomers of cellulose, and Congo Red. They concluded that the CD spectrum is the result of a chain length dependent association between the saccharide and the dye molecule. Although cellulose oligomers ranging from cellobiose through the hexamer were studied, they found no evidence for complexation with oligomers shorter than 5.[85] Since the dye is achiral and has no CD spectrum, and the methylcellulose or cellulose oligomer has no CD in the visible region, the authors postulated that the dye molecules adopt a dissymetric conformation when binding to the cellulose chain. There is a wealth of supporting evidence for this kind of interaction producing induced CD activity from studies of interactions of dyes and small drug molecules with polypeptides and proteins.[86] Experimental evidence for the existence of a helical conformation of polysaccharides in solution is apparently the subject of some debate in the literature. The best

evidence in support of this postulate appears to come from Yalpani who has data that support a right hand helical structure for amylose type polysaccharides and extended flat ribbon structures for the beta-glucans.[87]

Results from the present study augment the work done previously in terms of an increase in the number and types of dyes tested in order to determine what structural features, if any, are necessary for solution binding with cellulose type polysaccharides. Both dye types, those that are active in modifying the structure of *A. xylinum* cellulose, Table IV, and those that are inactive, (Table V), are included. In addition, data concerning the effects of chain length or degrees of polymerization (DP), the effects of changing the glycosidic linkage, and other structural modifications to the chiral substrate are included. Cellulose oligomers from cellobiose through the octamer were used, along with methylcellulose, hydroxypropylcellulose (HPC), soluble starch (amylose), and linear malto-oligosaccharides. Cyclodextrins were also included because of the widespread interest that they have generated as chiral stationary phases in chromatographic applications.[17] Equilibrium constants for several of the dye-oligosaccharide association reactions are reported for the active dyes, and possible structural features of the chiral complexes are discussed.

Experimental

Standard Materials

The cello-oligosaccharides (Figures 24 to 31) were prepared by Hyatt *et al.*[88] from fully acetylated derivatives. The procedure involves transesterification of the cellulose acetates with a catalytic amount of sodium methoxide in methanol at ambient temperature. The oligosaccharides were recrystallized from 95% ethanol and characterized in terms of melting point and optical rotation.[88]
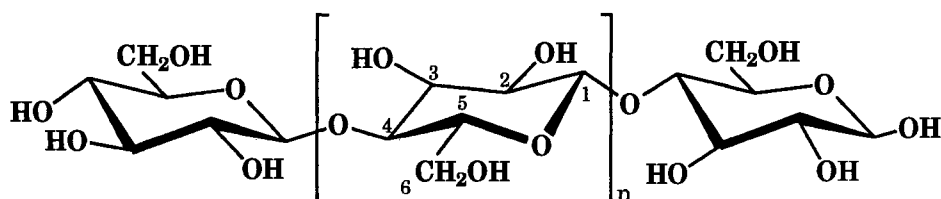
Figures 24-31. Structures of cellulose and its oligomers.

24. $n \approx 50$ (cellulose)
25. $n = 0$ (cellobiose)
26. $n = 1$ (cellotriose)
27. $n = 2$ (cellotetraose)
28. $n = 3$ (cellopentaose)
29. $n = 4$ (cellohexaose)
30. $n = 5$ (celloheptaose)
31. $n = 6$ (cellooctaose)

Cellobiose, methylcellulose, HPC, and the malto-oligosaccharides were purchased from Sigma Chemical Co. and were used without further purification. The β-cyclodextrin was obtained from Eastman Kodak Company, and the γ-cyclodextrin was the generous gift of American Maize

Company; both were used as received. Congo Red, (Table V), was twice recrystallized before use. All other dyes were commercial materials of certified purity.

Reagents

Stock solutions of the various dyes were prepared by dissolving the respective materials in pH 7.0 sodium potassium phosphate buffer (0.2 M ionic strength). Stock solutions of the cellulose oligomers or other host molecules were prepared using the dye stock solution, and successive dilutions were prepared by dilution of the stock host solutions with the dye stock. In this manner, a constant concentration of the dye was easily maintained.

Amylose and the hepta- and octamers of cellulose required heating to effect solution in the buffer. Methylcellulose was recalcitrant to the solution process in phosphate buffer, even after extended periods of heating.

Measurements

All measurements were made using the Jasco J-500A recording spectropolarimeter previously described. The wavelength range, sensitivity, scan rate, slit width, and accumulation times were selected to provide the optimum signal to noise ratios for each of the complexes. A cell path length of 1.0 cm was used for all measurements.

In order to establish the baseline, the actual wavelength range over which the CD spectrum of the complex was measured was wider than the range of the dye absorption spectrum. Since the J-500A is a single beam instrument, corrections for the cell blank and instrument baseline were made by subtracting the spectrum for the buffer.

The formation constants for the dye-saccharide complexes were determined by measuring the CD spectrum for a series of dilutions of the sugar. The solutions were prepared so that the dye concentration remained constant at 0.05 mM while the saccharide concentrations were systematically decreased. The dye concentration was held at a relatively low value to avoid excessive absorption, thereby staying within the dynamic range of the instrument. Saccharide concentrations were always in excess of 0.05 mM to ensure that the dye was the limiting reagent. Typically, spectra for six dilutions were measured over the concentration range of 0.10-10.0 mM. Concentrations in the upper range were necessary when molecular association reactions produced complexes with a weak CD signal.

Results and Discussion

The dyes in Table IV are known to be active in terms of their ability to prevent the assembly of crystalline cellulose by *A. xylinum*.[89] Solutions were prepared for each of these dyes in the presence of the following

substrates or hosts: methylcellulose, HPC, and the series of

oligosaccharides from cellobiose to cellooctaose.

Although Calcofluor white, (Table IV), was the first dye reported to

affect the formation of normal bacterial cellulose, the induced signals from

its association with the series of cello-oligomers were extremely small and

of poor quality in terms of the signal to noise (S/N) ratio; therefore,

formation constants could not be calculated. The other dye molecules

produced spectra of much higher quality. This is a consequence of a more

favorable molar ellipticity and is also a result of chromophores that absorb

in the visible region of the spectrum, away from the aromatic interferences,

leading to an increase in the S/N ratio (Figure 32).
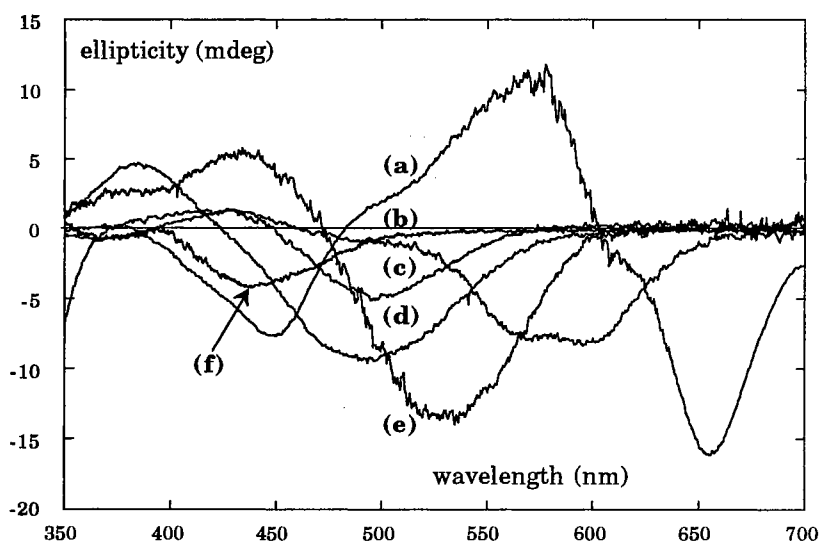
Figure 32. Induced CD spectra for complexes formed between cellohexaose and the direct dyes: (a) Trypan Blue, (b) Direct Violet No. 1, (c) Direct Yellow No. 1, (d) Direct Orange No. 8, (e) Congo Red, and (f) Titan Yellow at equimolar concentrations in aqueous pH 7.0 phosphate buffer.

The spectral features for all the induced CD spectra are similar. As one proceeds from longer to shorter wavelengths, the Cotton effect associated with the CD band at the longest wavelength is negative in sign and of higher intensity than the positive band immediately adjacent to it, which maximizes at a shorter wavelength. Under the essentially equimolar dye conditions as shown in Figure 32, the intensity of the induced CD spectrum for Trypan Blue, (a), is the largest in magnitude. For this particular dye, the negative and positive band maxima occur at much longer wavelengths than their counterparts. In addition, there is the appearance of a third major band at about 440 nm. This shorter wavelength negative band is also seen in Direct Violet and is probably present for all of the direct dyes. For the dye materials that absorb farther into the blue wavelength region, this band would be masked by the high background UV absorbance of the aromatic chromophores. CD spectra for a given dye, e.g. Congo Red, when complexed with the oligomers and analogs of the cellulose series are very similar (Figure 33) differing only in their relative intensities.

Cellotetraose was the shortest member of the homologous series for which there was substantial evidence for the molecular association reaction. A red shift of approximately 15 nm for the longest wavelength maximum is noted for the complex with HPC (Figure 33). Since the spectrum for the methylcellulose conforms with the spectra for the oligomers, the shift for HPC can probably be attributed to the involvement of
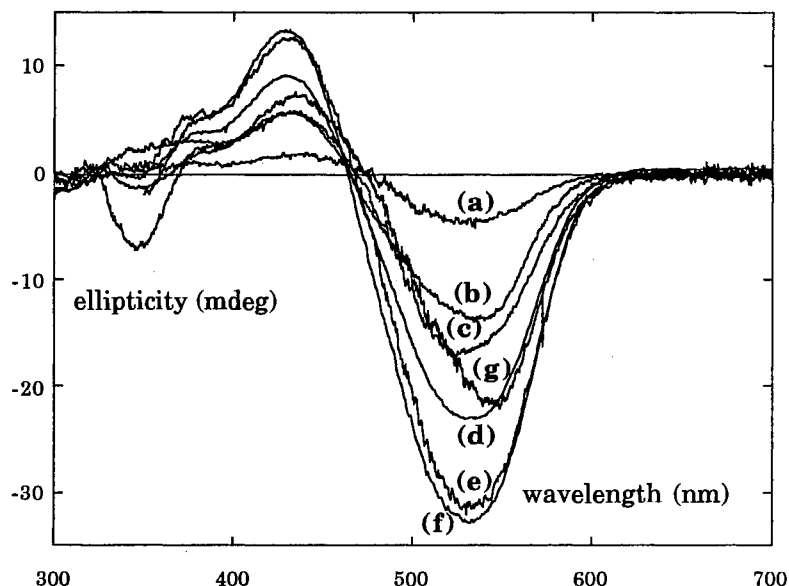
Figure 33. Induced CD spectra for complexes formed between Congo Red and (a) cellotetraose, (b) methylcellulose, (c) cellopentaose, (d) cellooctaose, (e) cellohexaose, (f) celloheptaose, and (g) hydroxypropylcellulose in pH 7.0 phosphate buffer. The oligomers are at equimolar concentrations. Concentrations of the polymers are not defined exactly because of uncertainty in the molar masses and the relative insolubility of (b).

either steric effects associated with the larger side chain and/or the -OH functional groups in the association mechanism.

The dyes in Table V were tested and found not to produce CD spectra with the celluloses. This list includes Nile Blue A and Light Green SF Yellowish that Haigler tested and reported as ineffective in altering the nature of *A. xylinum* produced cellulose, to any significant degree. There is an apparent correlation between the dyes that are capable of binding to crystalline cellulose and altering the morphology of bacterial cellulose and those that are capable of binding to cellulose oligomers, methylcellulose, and HPC in aqueous solution.

In addition to the cellulose type polysaccharides, Calcofluor and the direct dyes also bind to amylose and the related malto-oligomers as well as the β and γ cyclodextrins (Figures 34 & 35). The shortest malto-oligomer for which there was substantial positive evidence for CD induction was the hexamer. This is explained by the fact that, overall, the induced CD signals for the malto-oligomer series are much less intense than those for the equivalent member in the cello series for a given dye. A familiar CD spectral pattern exists much like in the cello series, but in this case, the inverse of the pattern is observed for the complexes; i.e., there is a positive inflection for the longest wavelength band, etc. As can be seen from the spectra in Figure 34, there is one, as of yet, unexplained exception to the
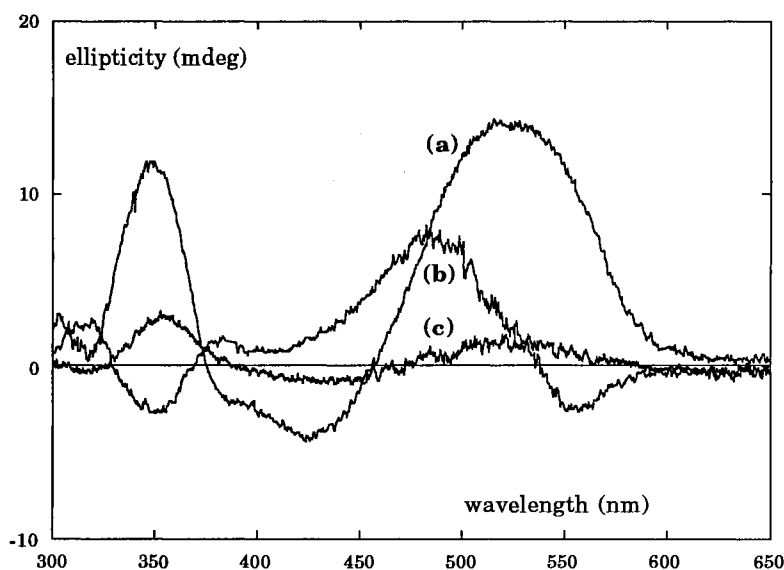
Figure 34. Induced CD spectra for complexes formed between Congo Red and (a) amylose, (b) maltoheptaose, and (c) maltohexaose in pH 7.0 phosphate buffer. The oligomers are at equimolar concentrations. The amylose concentration is not defined exactly because of the uncertainty in the molar mass.
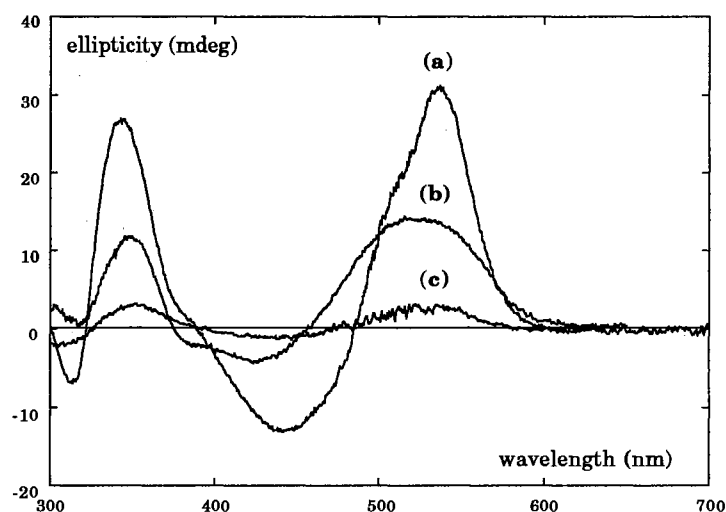
Figure 35. Induced CD spectra for complexes formed between Congo Red and (a) γ-cyclodextrin (0.14 mM), (b) amylose, and (c) β-cyclodextrin (2.78 mM) in pH 7.0 phosphate buffer.

series when complexed with Congo Red. The spectrum for the maltoheptaose-Congo Red complex shows a relatively large blue-shift, and a new, low intensity band appears that maximizes near 550 nm. The same spectrum was obtained using maltoheptaose samples from three separately purchased samples and is unlikely the result of contamination of the material after purchase.

The induced CD spectra observed in the visible range are due entirely to the complex formed. The observed intensity at any given wavelength, ψ_{DS}, is determined by two multiplicative factors. One factor is the number of dye molecules that are complexed, and the other factor is the induced rotational strength for the association complex. The formation constant, K_{DS}, is an expression of the extent to which the dye molecules are

complexed, and the induced rotational strength is proportional to the molar induced ellipticity θ_{DS}, where D, S, and DS refer to dye, sugar, and the complex respectively.

Since the measured signal size is proportional to the molar concentration of the formed complex, Beer's Law applies and the mathematical model of Benesi and Hildebrand[90] can be used to calculate K_{DS} for those systems where complexation occurred and where the chiral substrates or hosts were available in sufficient quantities to make a series of measurements possible. The model is predicated on the formation of a 1:1 complex in dilute solution. In order to calculate equilibrium constants using this model, the concentration of either the host or the guest (dye molecule) must be kept constant while the other is systematically changed.

The following equation (see Appendix A) gives the basis for the calculation of the formation constants

$$\frac{bC_D C_S}{\psi} = \frac{C_D + C_S - [DS]}{\theta_{DS}} + \frac{1}{K_{DS}\theta_{DS}} \tag{31}$$

where b is the path length; C_D and C_S are the analytical concentrations for the dye and saccharide, respectively; $[DS]$ is the equilibrium concentration for the complex; ψ is the measured ellipticity; θ_{DS} is the molar ellipticity; and K_{DS} is the formation constant for the complex.

Because both K_{DS} and θ_{DS} are unknown, the simultaneous solution is done by an iterative least squares procedure. The procedure is initiated by providing an initial guess for $[DS]$ (typically $[DS] = 0$). The first iteration

provides an approximate value for [DS], which becomes the initial guess for the next cycle. This process repeats until successive values for K_{DS} converge at a value that is within ± 10.[90],[91]

Spectra for a typical series of dilutions are shown for Congo Red, which is held at constant concentration with various concentrations of cellohexaose as shown in Figure 36. The spectral features remain similar as the carbohydrate concentration is increased. For these saccharide to dye ratios, where the dye is the limiting reagent, it is assumed that the stoichiometry of the complex formed is 1:1. This is a reasonable assumption and can be confirmed for molecules of low molecular weight. For high molecular mass substances such as methylcellulose, HPC, or amylose, one would expect the number of potential binding sites and the stoichiometry to
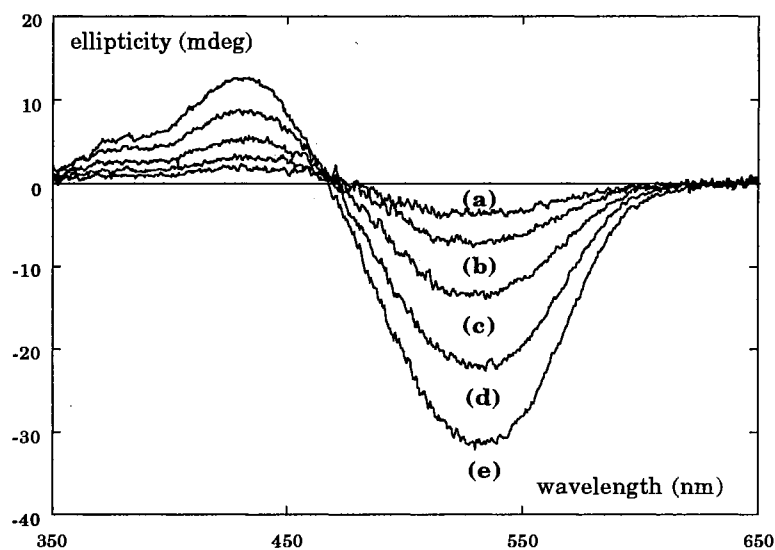
Figure 36. Induced CD spectra for solutions of Congo Red and cellohexaose as a function of the cellohexaose concentration (a) 0.17 mM, (b) 0.34 mM, (c) 1.37 mM, (d) 2.75 mM, and (e) 6.87 mM, in pH 7.0 phosphate buffer.

be greater than one. In order to compensate for uncertainties in the molar masses of these polymeric forms, and to incorporate the idea that a particular minimum repeat length is necessary for complexation, binding constants for HPC and starch amylose were calculated using analytical concentrations that were normalized in terms of the molar mass of the hexamer or heptamer as the repeating unit.

Calculated values for K_{DS} and θ_{DS} are given for the cellulose series in Table VI. Experimental data were taken at the wavelengths of the respective maxima for the most intense bands. While values for K_{DS} are directly comparable within and among different dye systems, θ_{DS} values are wavelength dependent and can only be compared for a given dye with a series of hosts.

The part of the study regarding the largest number of complexes involved Congo Red. In the series with the cello-oligomers, K_{DS} increases with the molar mass of the hosts and reaches a maximum value at the heptamer. Formation constants for the methylcellulose-dye complexes are missing because of the very limited solubility of methylcellulose in the phosphate buffer. The value reported for the Congo Red-HPC complex, (Table VI), was calculated using a stock solution concentration that was normalized to the molar mass of the heptamer. Under these conditions, it is more correctly referred to as a binding constant, and it differs from the K_{DS} value for the celloheptamer by only a factor of two. Molar ellipticities for the cello series appear to maximize at the pentamer or hexamer length. If the

Table VI. Formation Constants and Molar Ellipticities for Direct Dye Complexes with a Series of Cellulose Oligomers and Hydroxypropylcellulose (HPC)

Oligomer	-tetraose	-pentaose	-hexaose	-heptaose	-octaose	HPC**
Congo Red			(530nm)			
K_{DS}	40	100	410	995	1000	1800
θ_{DS}	-780	-1700	-1230	-940	-800	-400
Direct Orange No.8			(485nm)			
K_{DS}	-	120	400	830	-	-
θ_{DS}	-	-280	-280	-220	-	-
Direct Yellow No.1			(490nm)			
K_{DS}	-	-	700	-	-	-
θ_{DS}	-	-	-150	-	-	-
Direct Violet No.1			(595nm)			
K_{DS}	-	190	140	220	-	-
θ_{DS}	-	-80	-350	-290	-	-
Trypan Blue			(660nm)			
K_{DS}	-	-	2580	-	-	-
θ_{DS}	-	-	-510	-	-	-
Titan Yellow			(436nm)			
K_{DS}	-	-	498	-	-	-
θ_{DS}	-	-	-152	-	-	-

** Formula weight normalized to the heptamer (1765 g/mole)

magnitude of the induced rotatory strength is an indication of the space-filling efficiency of the molecular fit, a possible conclusion to be drawn from this is that the molecular dimensions of the dye and the saccharide are such that the complex is favored when the saccharide is of this minimum length. For the HPC-Congo Red complex, the resultant θ_{DS} is independent

of whether the concentrations of the HPC dilutions are calculated using the molar mass for the hexamer or the heptamer, since the minimum chain length condition has been met.

Comparison between the malto-series and the cello-series, when complexed with Congo Red, shows that the maltoses produce CD spectra that are much less intense. As a result of this effect, the only maltose with signals large enough to calculate values for θ_{DS} and K_{DS}, with any degree of confidence, was the heptamer, (Table VII).

Table VII. Formation Constants and Molar Ellipticities for Congo Red and Direct Yellow No. 1 Complexes with a Series of Maltoses

Oligomer	maltoheptaose	ß-cyclodextrin	γ-cyclodextrin	amylose**
Congo Red	(470nm)	(530nm)	(530nm)	(530nm)
K_{DS}	26	36	44600	1970
θ_{DS}	250	700	760	420
Direct Yellow No. 1				
K_{DS}	-	-	700	-
θ_{DS}	-	-	7100	-

** Formula weight normalized to the heptamer (1155 g/mole)

A weak complex of comparable stability is formed between Congo-Red and the other maltoheptaose, namely, β-cyclodextrin. There is a real molar ellipticity difference, however, that can most likely be explained by the effects on the overall chirality of the saccharide from the added rigidity of the cyclic structure over the more open or extended structure. The complex with γ-cyclodextrin is the most stable of all of the maltose complexes. Interestingly, θ_{DS} values for the two cyclodextrins are strikingly similar in magnitude, so the huge difference in intensities of the measured ellipticities for the complexes are thermodynamic in origin as is evidenced by the large difference in the calculated values for the formation constants. The spectrum for the starch-amylose complex is similar to those for maltohexaose and the cyclodextrins. It does show some loss of structure and a small shift towards the blue in the longest wavelength band, along with some evidence of structure in the negative band. The positive Cotton effect, which maximizes at ~340 nm, is present in all three spectra. When the amylose concentration is expressed in terms of the molar mass of the heptamer, the binding constant is two orders of magnitude greater than that for the maltoheptaose formation constant. However, as in the case with Congo Red and the cello-oligomers, the molar ellipticities are comparable in magnitude.

Calculations for the other direct dyes with the cello-series are somewhat limited due to the limited quantities of some of the sugars. Data from Direct Orange #8 and Direct Violet #1 are fairly complete, however,

and the trends in the values for K_{DS} and θ_{DS} that were observed for Congo Red appear to be repeated. Evidence for a complexation with cellotetraose for dyes other than Congo Red was observed, but poor S/N ratio prevented the calculation of K_{DS} and θ_{DS}.

All formation constants that were calculated for the active dyes in Table IV are included in Table VI. In comparing the dyes, there appear to be no obvious systematic structural differences that would account for the wide range in values for K_{DS} and θ_{DS}. There are several potential sites on the dyes for hydrogen bonding to occur because all of the dyes have polar substituents, but only Trypan Blue has extra non-polar substituents. The presence of these extra functional groups might be the most significant factor that causes its complex with cellohexaose to have the greatest stability and perhaps provide an indication of the relative importance of hydrophobic interactions that are commonplace in binding to the cyclodextrins. An additional factor may be the degree of linearity inherent to the dye. For instance, of the remaining dyes, Direct Violet #1 has the least linearity and forms the least stable complexes, while Direct Yellow #1 is the most linear and forms complexes of the highest stability.

With Titan Yellow as the lone exception, the dyes that bind are structurally similar in that they all have three aromatic moieties disposed at separation distances of ca. 10.5 Å along a rigid bis-diazo-pseudolinear structure that is centered around a biphenyl functional group. The single bond linking the biphenyl rings would allow for some restricted rotation

about the molecular "halves." This could be the most important structural feature that allows the direct dyes to bind to the saccharide backbone in lieu of the other dye types. The central N-N σ-bond in the Titan Yellow molecule also allows some rotational freedom. The linear separations between adjacent aromatic groups closely match the separation between cellobiose units in the cellulose structure and, to a first approximation, the size and helical extension of the cellohexaose structure could approach the optimum combination necessary to bind fully with a dye such as Congo Red, Table IV. A shorter cellulose oligomer would have a minimum of one terminal dye aromatic ring system unassociated, which would result in a correspondingly lowered stability for the complex. Longer analogs would likely show a decreased stability as well because of the extra monomeric units that would not contribute to the formation of the complex. At some point, where additional monomeric units result in a chain length somewhat greater than the octamer, the polymer would undoubtedly be able to bind an additional dye molecule, although this would be difficult to test for in the cello-oligomers due to the poor solubility of the octamer in aqueous buffer.

Consistent with this argument of a necessary minimum host chain length for a complex of maximum stability is the observation that the formation constants for complexes of the cello-oligomer series maximize around the heptamer and the value for HPC, which is normalized to a repeating unit based on the molecular weight of the heptamer, is similar.

This observed "maximum" in the formation constant is in keeping with the idea that the origins of the extrinsic CD lie in the proposed helical structure of the chiral host and that, after one complete turn of the helix, there is little additional stabilization of the local dye-saccharide association complex. Given sufficient solubility, additional dye molecules that would bind to a long polymer would likely produce identical yet independent rotational events. Furthermore, there are no significant spectral changes observed with increasing molar mass so there is no evidence for *intermolecular* dye-dye interactions: cf. the spectral similarities mentioned before for the starch and the malto-series. While this interpretation of the induced CD activity does rely on a helical structure for the saccharide host, it does not establish its conformation as helical prior to complexation. Although there is no consensus concerning the existence of helical conformations for celluloses in solution, the experimental evidence seems to support some type of organized conformation. Lewis[63] has described the cyclodextrins as helical structures of amylose with zero pitch. This would lend some credence to the view of a helical structure for the celloheptaose due to the spectral similarities between it and β-cyclodextrin and that the effects of the end groups are apparently small.

Assuming that the dye-saccharide complexes do assume a helical configuration in solution, the reversal of sign for the induced CD signals when the same dye is complexed with a maltose versus a cellulose derivative would indicate opposite handedness for the helical forms in

solution.[87] By relating the bi-signate structures of the CD spectra to *intra*-molecular exciton coupling theories between aromatic chromophores in the dyes, the question of the handedness of the turn might be resolved. This interpretation of exciton coupling theory employs the concept that the dye molecules will rotate around the single sigma bond of the biphenyl moiety as it is "guided" by the helix. Exciton coupling theories propose a clockwise dihedral angle between the principal long rotation axes of the aromatic chromophores when the signs of the bands are positive to negative when progressing from long to short wavelength, and vice versa.[64] Providing that this is applicable to collinear dye moieties, which are able to assume the conformation of the substrate, it is a reasonable conclusion that the starch molecule possesses the clockwise conformation, as is coincident with the assignment by Yalpani,[87] and the helical rotation of the celluloses would be counter-clockwise.

Although the details of the precise mechanism of the dye-saccharide binding interactions have yet to be determined, there is experimental precedent that favors a mechanism based on hydrophobic interactions between aromatic species with saccharides in aqueous media.[92] The formation constant information provided by the current study is in agreement with this type of mechanism. Induced CD spectra are observed for the dyes with cello-oligosaccharides in water, but not in dimethylsulfoxide. If the sugars and dyes were linked by specific hydrogen-bonding interactions, then one would expect to see association even in

solvents less polar than water. Attempts to diminish the binding by the addition of the anti-hydrophobic agents urea and guanidinium chloride were non-quantitative. The large amounts required would overcome the capacity of the buffer, and the accompanying pH change would alter the degree of ionization and ultimately the binding of the dye molecules. Additionally, the dyes that bind to the sugars show great variation in the placement and type of solubilizing groups present. These attributes make it unlikely that hydrophilic interactions have to be specific in order to join the two species in aqueous solution.

Cyclodextrin-benzenoid complexes are not unique in the manner in which they form association complexes through hydrophobic interactions.[67,93] Many enzymes involved in sugar recognition and transport bear active sites in which aromatic rings stack on sugar rings.[94,95] An example is the maltodextrin binding protein of *E. coli*, which fixes maltose between four amino acid aromatic side chains.[96] It is also possible that the binding of the fungal cellulase, cellobiohydrolase I from the wood-destroying organism *Trichoderma reesei*, may occur by a hydrophobic mechanism. This organism has been studied in detail[70,72,74] and has been shown to consist of a small (37 residue) cellulose-binding domain that is linked to a large glycoside-cleaving domain. The three-dimensional structure of the cellulose binding domain of this enzyme[73] possesses a coplanar array of three aromatic (tyrosine) residues with each of the three benzene ring centers separated by about 10.4 Å. This is exactly

the disposition of the aromatic rings in dyes that bind to the cello-oligosaccharides. In addition, the association constants reported for the binding of the various cellobiohydrolases to cello-oligomers range from 730 to 62,000.[97,98,99] These values are reasonably consistent with the constants obtained in this study for the dye-oligomer complexes. Similarly, it is reasonable to expect a hydrophobic association between the aromatic rings of the dye and the C-H units of positions labeled as 2, 4, 1', 3', and 5' of the cellobiose repeat unit in the glucan chain (Figure 37). This model was constructed based on conformational data derived from X-ray analysis of crystalline cellulose I[100] and a model of Congo Red superimposed upon the labeled sites.

Figure 37. Space-filling model of a plausible structure for the complex between cellulose I and Congo Red illustrating its specific involvement with the hydrogens in the C2, C4, C1', C3', and C5' positions of the cellobiose repeat unit of the glycan chain.

In summary, the dyes that were reported to bind to and significantly alter the crystalline nature of bacterial cellulose pellicles are also capable of binding to cello-oligomers in bulk, aqueous medium. The CD data from the

dye-saccharide complexes provides evidence for the existence of preferred helical conformations for polymeric saccharides as well as oligosaccharides of cellulose and maltose in aqueous solution. The opposite signs observed for the induced CD spectra for the maltose and cellulose series suggest that the helices turn in opposite angular directions. This is most likely attributable to control by the different stereochemistries about the C1-C4' linkages between monomeric units.

The results from using the binding of dye molecules as a structural probe to determine molecular conformations of carbohydrates in solution is in agreement with the conclusions reached for the far-UV studies of the underivatized sugars. The visible range is experimentally much more convenient to use and is a complement to the UV studies. CD induction by complexation reactions have much potential and should be further exploited as an analytical tool for structural and conformational studies. The mechanism for the binding process is likely hydrophobic in nature, consistent with the results from molecular association reactions with cyclodextrin molecules and proteins.

CHAPTER VI

A POTENTIAL ROLE FOR CIRCULAR DICHROISM IN CHIRAL RECOGNITION OF INTERMEDIATES IN BIOSYNTHETIC PATHWAYS

Introduction

Secondary products are substances that plants produce in response to herbivore or pathogen attack. There are three primary groups of these natural products: alkaloids, terpenes, and the phenolic compounds. Groups are classified based on biosynthetic criteria that include well defined biosynthetic pathways and precursors from primary metabolism. The pathways that result in the formation of the various secondary products are known as the shikimic acid, mevalonic acid, and malonic acid pathways.[101]

The flavonoids are a particular subset of the phenolic compounds produced via the actions of the shikimic and malonic acid pathways as shown in Figure 38. Figure 39 is descriptive of the basic flavonoid nucleus that is an end product of these processes. The three-carbon bridge and the phenyl group B are synthesized by way of the shikimic acid pathway. The other aromatic ring results from the involvement of three acetate units via the malonic acid pathway.[101]

Erythrose 4-phosphate
(from pentose phosphate pathway

Phosphoenolpyruvic acid
(from glycolysis)

Shikimic Acid
Pathway

Acetyl CoA

◯—CH₂CHCOOH
　　　|
　　　NH₂

Phenylalanine

Malonic Acid
Pathway

◯—CH=CHCOOH

Cinnamic acid

simple phenolics
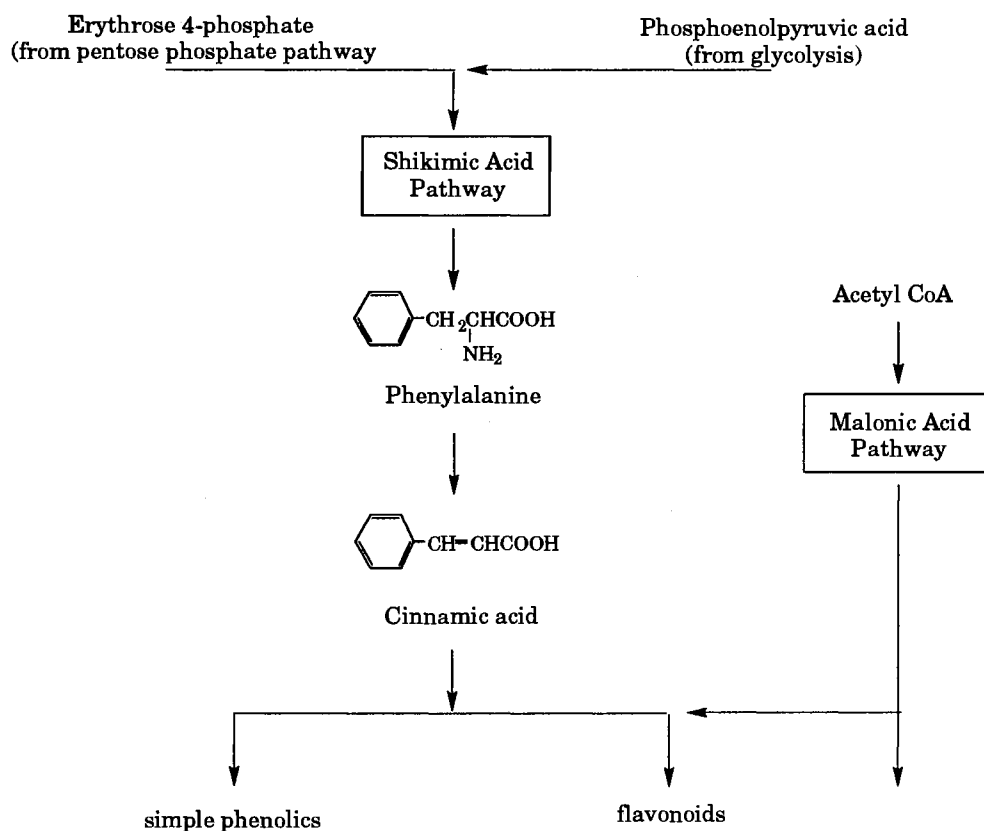
flavonoids

Figure 38. Biosynthesis of plant phenolics (adapted from reference 101).

From malonic
acid pathway

From shikimic acid
pathway via
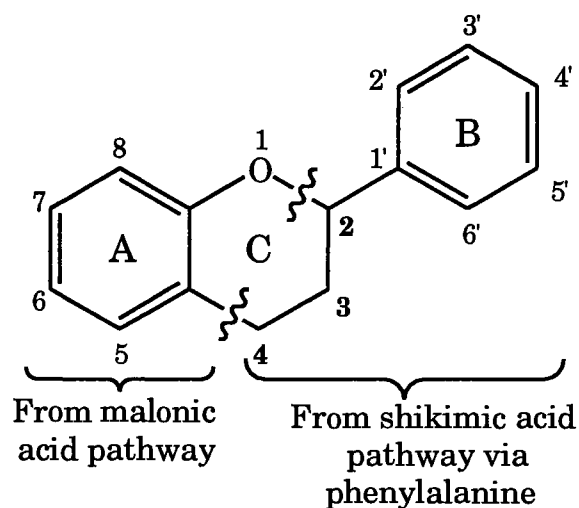phenylalanine

Figure 39. The numbering system for the flavonoid nucleus (adapted from reference 101).

Flavonoids are classified into at least four major divisions based primarily on the degree of oxidation and substitution at the B precursor (Fig. 39) that forms the three-carbon bridge of the basic flavonoid structure. The four divisions are anthocyanins, flavones, flavonols, and isoflavonoids.[101] If the aromatic ring B is shifted from position two to position three (Fig. 39), the resulting structure is of the isoflavonoid type, which is a particularly large and distinctive subclass of the flavonoids. The isoflavonoids include a number of other groups such as the isoflavones, rotenoids, and pterocarpans.[102] Many of the isoflavonoids are known to be phytoalexins, the compounds responsible for antifungal and antibacterial bio-responses to pathogen infection.[101]

Phytoalexins are synthesized rapidly following bacterial or fungal attack. Prior to attack, they are generally undetectable, but they appear in high concentrations within hours following infection. They are toxic to a broad spectrum of plant pathogens, both bacterial and fungal, and help to limit the spread of the pathogenic organism. Although different plant families produce phytoalexins related to different groups of the secondary plant products, the legume family produces phytoalexins that are isoflavonoid derivatives.[101] One of the major isoflavonoid phytoalexins produced by legumes, such as alfalfa (*Medicago sativa*)[103] and peanut (*Arachis hypogaea*),[104] is the antifungal pterocarpan known as medicarpin (Figure 40).
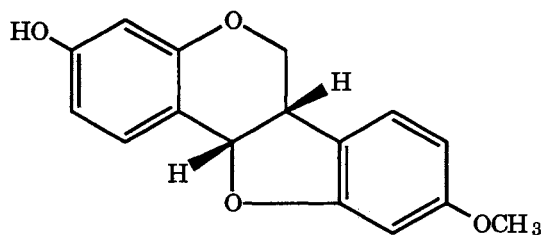
Figure 40. Structure of medicarpin; the (+)-enantiomer is shown.

As can be seen from Figure 41, the chiral centers at positions 6a and 11a that join the fused ring system B/C determine the stereochemistry of the pterocarpans. The two medicarpin isomers that are thought to occur naturally are the (-)- and (+)-forms, known biochemically as (6aR,11aR)-medicarpin and (6aS,11aS)-medicarpin, respectively. Strange and Ingham extracted and purified pterocarpans from peanut leaflets, which they believed to be medicarpins. Optical activity measurements revealed that the pterocarpan they isolated was dextrorotatory. Based on this information, and information from TLC and mass spectral data, they identified the pterocarpan as the 6aS,11aS or (+)-medicarpin enantiomer (Fig. 40). This is

Figure 41. The numbering system for the pterocarpan nucleus (adapted from reference 102).

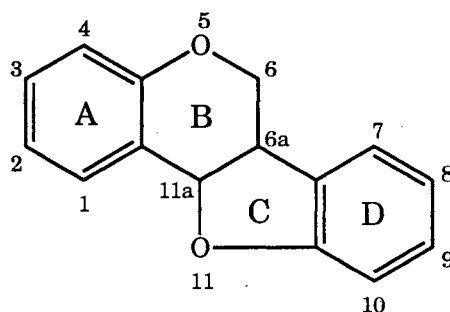an unusual result in that the pterocarpans with a hydrogen substituent at the 6a position are typically levorotatory.[104]

In general, it has been shown that the stereochemistry of the end product of pterocarpan synthesis can be very important in determining the extent of the isomer's antifungal properties, since some fungi are reported to possess detoxification mechanisms that are stereospecific to a particular pterocarpan isomer.[105] For example, studies of the pterocarpans, (+)- and (-)-maackiain, produced by red clover showed greater antifungal activity for the (+)-isomer.[106]

An understanding of the pathways for medicarpin biosynthesis are essential to interpreting the disease resistance properties of isoflavonoids and related substances as well as for potential manipulation of the phytoalexin pathway via gene transfer technologies.[103] Dixon and Paiva have initiated such a study in order to understand the molecular biology of alfalfa defense responses. The portion of the biosynthetic pathway that they have proposed for the biosynthesis of (-)-medicarpin, based on characterization of the specific enzymes involved for production of related isoflavonoids in soybean, chickpea, and pea, is illustrated in Figure 42.[103]

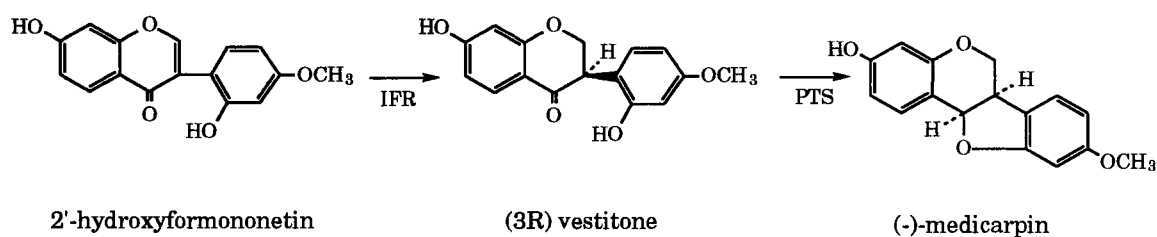2'-hydroxyformononetin   (3R) vestitone   (-)-medicarpin

Figure 42. Biosynthesis of (-)-medicarpin in alfalfa from achiral precursor.

The early emphasis in investigation of the phytoalexin defense response and its regulation in alfalfa has involved the enzymes that act late in the biosynthesis of medicarpin. Phenylalanine, an end product of the shikimic acid pathway, plus three malonic acid residues[101] are the precursors to intermediate flavones, which give rise to the achiral isoflavonoid intermediate 2'-hydroxyformononetin. This undergoes a reduction by isoflavone reductase (IFR) to form the chiral intermediate (3R) vestitone. This intermediate is then acted upon by pterocarpan synthase (PTS), with no change in 6a stereochemistry, to form the pterocarpan phytoalexin, (-)-medicarpin.[107]

For confirmation of the relative stereochemistry of the intermediates, as they are isolated along the biosynthetic pathway, CD spectropolarimetry can provide important qualitative information. What follows is a discussion of exploratory work to evaluate the technique as a method to test for the expression of chiral molecular characteristics following transgenic mutation; i.e., genetic manipulation to produce an alfalfa or other host organism containing IFR and PTS enzymes that form (+)-medicarpin.

Experimental

Materials and Methods

All medicarpin and vestitone samples were provided by The Noble Foundation, Ardmore, Oklahoma. The medicarpins were obtained from

alfalfa cell cultures and peanut plants and extracted and prepared according to the procedure outlined by Dixon.[103] Samples were dissolved in methanol and dilutions were prepared as necessary to optimize the signal with regard to background absorbance.

CD Measurements

CD spectra were recorded for the isoflavonoid intermediates (vestitones) and medicarpins using the JASCO J-500A described previously. Data acquisition included the range from 220-400 nm. The sensitivity, scan rate, slit width, and accumulation times were selected to provide the optimum signal-to-noise ratios for each of the samples. Typical instrumental parameters used were sensitivity of 10, scan rate of 100 nm/min, slit width of 1.0 mm, and 8 accumulation times. A cell path length of 1.0 cm was used for all measurements unless otherwise noted.

Results and Discussion

Figure 43 shows CD spectra of vestitone extracts from alfalfa and from peanut leaves. If the pathway in Fig. 42 is complete, then it would be a reasonable presumption that the stereochemistry of the vestitone would ultimately play a role in the stereochemistry of the medicarpin; i.e., (3R) vestitone should form (-)-medicarpin and vice versa. The vestitone spectra from both alfalfa and peanut extracts are identical in terms of band
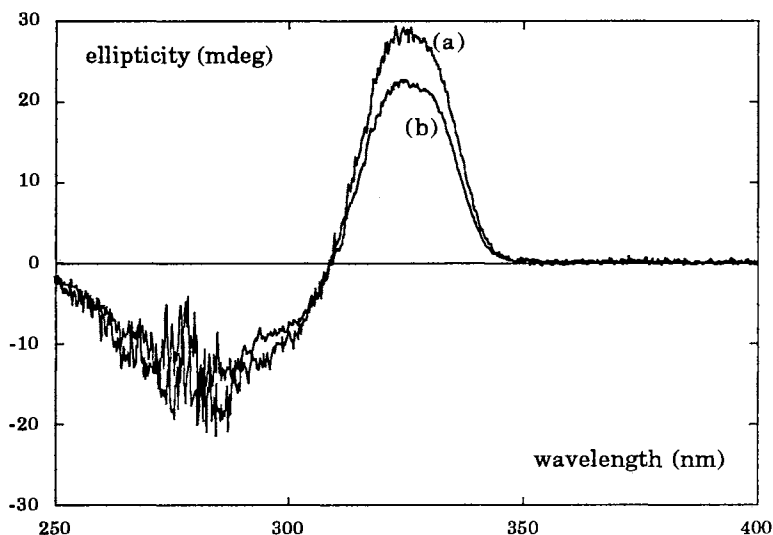
Figure 43. Circular dichroism spectra of vestitone extracts for (a) peanut and (b) alfalfa (2 cm cell).

placement and sign, differing only in magnitude due to different concentrations.

Since the CD spectra in Figure 44 for the medicarpin extracts from peanut and alfalfa are mirror-images, consistent with the work of Strange and others, there has to have been a loss of chiral integrity at position 6a for one of the syntheses. Two explanations for the formation of what appear to be enantiomers of medicarpin from (3R) vestitone are possible. One explanation is that an additional epimerization step has occurred after the (3S) vestitone is formed. This would result in the transformation of (3S) vestitone to its counterpart (3R) vestitone before undergoing the PTS reaction.[108] A second explanation lies in the particular stereochemistry about the B/C fused ring system. While it is likely that there is a step
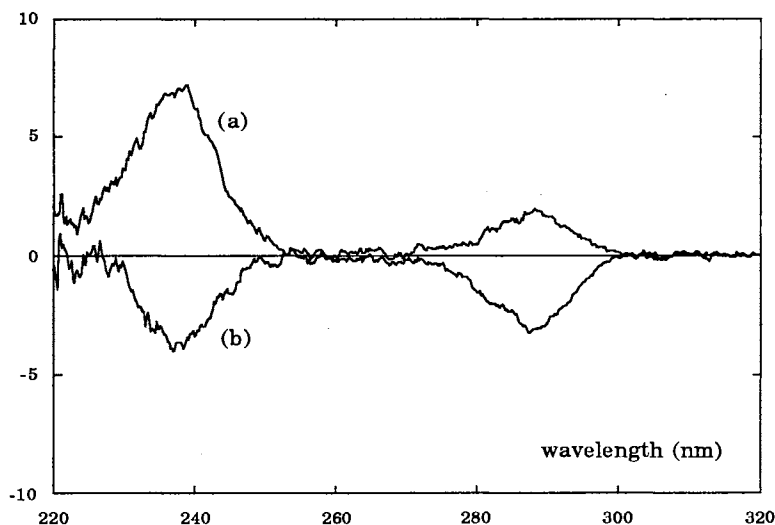
Figure 44. Circular dichroism spectra of medicarpin extracts for (a) peanut and (b) alfalfa.

subsequent to the formation of vestitone, the result might be the formation of either isomer of the 6aR,11aS or 6aS,11aR enantiomeric pair, each isomer of which would be diastereoisomeric to either the 6aR,11aR or 6aS, 11aS medicarpin. This occurrence of adjacent chiral centers is much like the stereochemistry found in the family of ephedrines. If one of the two diastereoisomers is formed, it is impossible to distinguish this medicarpin from either of the R,R or S,S enantiomers based upon the evidence from their native CD spectra alone; cf. for the ephedrines (-)EPH and LSF there are no unique spectral features to allow for differentiation among these enantiomers and the diastereoisomers (Figure 12). Although theoretical studies have shown that a ring fusion resulting in an R,S or S,R configuration for pterocarpans is, in general, not thermodynamically

favorable,[109] this type of bridge is not unique to the pterocarpans. For example, some rotenoids possess a B/C ring junction for which both the *cis-* and *trans-* forms are thermodynamically stable.[102] It is this type of situation for which a chiral induction reaction could augment the selectivity of the CD detector as a method for qualitative analysis of products following genetic manipulation.

CD has the potential to be a powerful tool for monitoring the relative stereochemistries of biosynthetic intermediates, but to use CD effectively for following chiral intermediates that have adjacent asymmetrical centers, it may be necessary to employ a chiral induction reaction of some sort to obtain the necessary qualitative information. This approach was successfully applied in the analysis of binary mixtures of diastereoisomers of ephedrines, as the four isomers produced unique spectra when complexed with the modified biuret reagent based on copper *l*-tartrate (Figure 13).

Further research is needed to find additional chiral induction reactions for CD that will allow for discriminating between enantiomers and diastereoisomers for those compounds that possess adjacent chiral centers. This will increase the value of CD as it is used specifically for monitoring biochemical intermediates in the areas of molecular biology and genetic engineering.

LITERATURE CITED

(1)   *Analytical Applications of Circular Dichroism*; Purdie, N.; Brittain, H. G., Eds.; Elsiver:Amsterdam, 1994; Vol. 14.

(2)   Purdie, N.; Swallows, K. A.; Murphy, L. H. *Trends Anal. Chem.* **1990**, *9*, 136-142.

(3)   Crabbe', P. *ORD and CD in Chemistry and Biochemistry*; Academic Press, Inc.:New York, 1972.

(4)   Lowry, T. M. *Optical Rotatory Power*; Dover Publications, Inc.:New York, 1964.

(5)   Velluz, L.; Legrand, M.; Grosjean, M. *Optical Circular Dichroism: Principles, Measurements, and Applications*; Academic Press, Inc.:New York, 1965.

(6)   Lambert, J. B.; Shurvell, H. F.; Verbilt, L.; Cooks, R. G.; Stout, G. H. *Organic Structural Analysis*; Macmillan:New York, 1976.

(7)   Crabbe', P. *Optical Rotatory Dispersion and Circular Dichroism in Organic Chemistry*; Holden-Day:San Francisco, 1965.

(8)   Armstrong, D. W. *Anal. Chem.* **1987**, *59*, 84A-91A.

(9)   Djerassi, C. *Optical Rotatory Dispersion: Applications to Organic Chemistry*; McGraw-Hill:New York, 1960.

(10) Duffield, J. J.; Abu-Shumays, A. *Anal. Chem.* **1966**, *38*, 29A-58A.

(11) *Chiroptical Techniques: Nomenclature, Symbols, Units* (recommended); Spectroscopic Nomenclature Committee. International Union of Pure and Applied Chemistry.

(12) Hughes, H. K.; Barnes, R. B.; Bedell, H. M.; Bell, R. H.; Brice, B. A.; Brode, W. R.; Buc, G. L.; Canada, A. H.; Churchill, J. R.; Geffner, J.; Gilmore, J.; Guettel, C. L.; Harrison, G. R.; Lighty, P. E.; Roller, D.; Rosenbaum, E. J.; Scribner, B. F.; Steele, S. D.; Warga, M. *Anal. Chem.* **1952**, *24*, 1349-1354.

(13) *Model J-500 Automatic Recording Spectropolarimeter Instruction Manual*, Japan Spectroscopic Co., Ltd.:Tokyo, 1979.

(14) *Extra Pharmacopoeia*; 25 ed.; Todd, R. G., Ed.; The Pharmaceutical Press:London, 1967.

(15) Stinson, S. C. *Chem. Eng. News* **1993**, *71*, 38.

(16) De Camp, W. H. *Chirality* **1989**, *1*, 2-6.

(17) *Special Issue on: Chiral Discrimination*, Fell, A. F., Ed.; *Trends Anal. Chem.* **1993**, *12*, 125-189.

(18) Reitsma, B. H.; Yeung, E. S. *J. Chromatogr* **1986**, *362*, 353-362.

(19) Mannschreck, M. *Trends Anal. Chem.* **1993**, *12*, 220-225.

(20) Otsuka, K.; Terabe, S. *Trends Anal. Chem.* **1993**, *12*, 125-130.

(21) Gasparrini, D.; Misti, D.; Villani, C. *Trends Anal. Chem.* **1993**, *12*, 137-144.

(22) Yeung, E. S.; Synovec, R. E. *Anal. Chem.* **1986**, *58*, 1237A-1256A.

(23) Purdie, N.; Swallows, K. A. *Anal. Chem.* **1989**, *61*, 77-89A.

(24) Armstrong, D. W.; Zukowski, J.; Yubing, T.; Berthod, A. *Anal. Chim. Acta* **1992**, *258*, 83-92.

(25) Engle, A. R. M.S. Thesis, Oklahoma State University, 1990.

(26) Gornall, A. G.; Bardawill, C. J.; David, M. M. *J. Biol. Chem.* **1949**, *177*, 751-766.

(27) Agrawal, J. K.; Harmalkar, S. G.; Vijayavargiya, R. *Microchemical Journal* **1976**, *21*, 202-208.

(28) *Selected Methods for the Small Clinical Chemistry Laboratory*; Faulkner, W. R., Ed.; American Association for Clinical Chemistry:Washington, D.C., 1982; Vol. 9.

(29) *Advances in Chromatography*; Davankov, V. A., Ed.; Marcel Dekker:New York, 1980; Vol. 18.

(30) *The Merck Index of Chemicals and Drugs*; 7th ed.; Stetcher, P. G.; Finkel, M. J.; Siegmund, O. H.; Szafranski, B. M., Eds.; Merck & Co., Inc.:Rathway, N. J., 1960.

(31) Tyler, V. E.; Brady, L. R.; Robbers, J. E. *Pharmacognosy;* 8th ed.; Lea & Febiger:Philadelphia, 1981.

(32) Silverstein, R. M.; Bassler, C. G.; Morrill, T. C. *Spectrometric Identification of Organic Compounds*; John Wiley & Sons:New York, 1981.

(33) Cotton, F. A.; Wilkinson, G.; Gaus, P. L. *Basic Inorganic Chemistry;* 2nd ed.; John Wiley & Sons:New York, 1987.

(34) Mortimer, G. *Mathematics for Physical Chemistry*; Macmillan:New York, 1981.

(35) Geladi, P.; Kowalski, B. R. *Anal. Chim. Acta* **1986**, *185*, 1-17.

(36) Beebe, K. R.; Kowalski, B. R. *Anal. Chem.* **1987**, *59*, 1007A-1017A.

(37) Martens, H.; Naes, T. *Multivariate Analysis*; John Wiley & Sons:Chichester, 1989.

(38) Haaland, D. M.; Thomas, E. V. *Anal. Chem.* **1988**, *60*, 1193-1202.

(39) Anderson, R. L. *Practical Statistics for Analytical Chemists*; Van Nostrand Reinhold Company:New York, 1987.

(40) Malinowski, E. R.; Howery, D. G. *Factor Analysis in Chemistry*; John Wiley & Sons:New York, 1980.

(41) Mark, H. In *Handbook of Near-Infrared Analysis*; D. A. Burns and E. W. Ciurczak, Eds.; Marcel Dekker, Inc.:New York, 1992; Vol. 13.

(42) Wold, H. In *Multivariate Analysis*; P. R. Krishnaiah, Ed.; Academic Press:New York, 1966.

(43) Martell, A. E.; Sillen, L. G. *Stability Constants*; The Chemical Society:London, 1964.

(44) Bukhari, S. T. K.; Guthrie, R. D.; Scott, A. I.; Wrixon, A. D. *Tetrahedron* **1970**, *26*, 3653-3659.

(45) Caldin, E. F. *Fast Reactions in Solution*; Blackwell Scientific Publications:Oxford, 1964.

(46) Földi, Z.; Földi, T.; Földi, A. *Chemistry and Industry* **1955**, *41*,1297-1299.

(47) Peggion, E.; Palumbo, M.; Cosani, M.; Terbojevich, M. *J. Am. Chem. Soc.* **1977**, *99*, 939-41.

(48) Johnson, W. C. J. In *Advances in Carbohydrate Chemistry and Biochemistry*; Academic Press:New York, 1987; Vol. 45; pp 73-124.

(49) Ingle, J. D.; Crouch, S. R. *Spectrochemical Analysis*; Prentice Hall:Englewood Cliffs, NJ, 1988.

(50) Cheng, K. L.; Young, V. Y. In *Instrumental Analysis*; G. D. Christian and J. E. O'Reilly, Eds.; Allyn and Bacon, Inc.:Boston, 1986.

(51) *MathCAD*, MathSoft, Inc.:Cambridge, 1989.

(52) Schwartz, L. M. *Anal. Chem.* **1976**, *48*, 2287-2289.

(53) Brown, P. J. *Analytical Proceedings* **1990**, *27*, 303-306.

(54) *Systems Under Indirect Observation*; Joreskog, K. G.; Wold, H., Eds.; North-Holland Publishing Company:Amsterdam, 1982; Vol. 139.

(55) Kelly, J. J.; Callis, J. B. *Anal. Chem.* **1990**, *62*, 1441-1451.

(56) Jensen, R.; Peuchant, E.; Salles, C. *Anal. Chem.* **1987**, *59*, 1816-1819.

(57) Dubois, P.; Martinez, J. R.; Levillain, P. *Analyst* **1987**, *112*, 1675-1679.

(58) Bjorsvik, H.; Bye, E. *Appl. Spectrosc.* **1991**, *45*, 771-778.

(59) Wegscheider, W.; Otto, M. *Anal. Chem.* **1985**, *57*, 63-69.

(60) *Unscrambler User's Guide*, CAMO A/S:Trondheim, 1993.

(61) Nevell, T. P.; Zeronian, S. H. In *Cellulose Chemistry and Its Applications*; T. P. Nevell and S. H. Zeronian, Eds.; Ellis Horwood Limited:Chichester, 1985.

(62) Lehninger, A. L. *Principles of Biochemistry*; Worth Publishers Inc.:New York, 1982.

(63) Lewis, D. G.; Johnson, W. C. J. *Biopolymers* **1978**, *17*, 1439-1449.

(64) Harada, H.; Nakanishi, K. *Circular Dichroic Spectroscopy, Exciton Coupling in Organic Stereochemistry*; University Science Books:Mill Valley, CA, 1983.

(65) Wiesler, W. T.; Nakanishi, K. *Croat. Chem. Acta* **1989**, *62*, 211-226.

(66) Banks, W.; Greenwood, C. T. *Polymer* **1971**, *12*, 141-144.

(67) Szejtli, J. *Cyclodextrin Technology*; Kluwer Academic Publishers:Dordrecht, 1988.

(68) *Eastman Cellulose Esters*, Eastman Kodak: 1991; Publication No. E-146K.

(69) Wood, P. J. *Carbohydrate Res.* **1980**, *85*, 271-287.

(70) *Biosynthesis and Biodegradation of Cellulose*; Haigler, C. H.; Weimer, P. J., Eds.; Marcel Dekker, Inc.:New York, 1991.

(71) *Cellulosics: Chemical, Biochemical, and Material Aspects*; Kennedy, J. F.; Phillips, G. O.; Williams, P. A., Eds.; Ellis Horwood:New York, 1993.

(72) Johansson, G.; Stahlberg, J.; Lindeberg, G.; Engstrom, A.; Pettersson, G. *FEBS Lett.* **1989**, *243*, 389-393.

(73) Kraulis, P. J.; Clore, G. M.; Nilges, M.; Jones, A.; Pettersson, G.; Knowles, J.; Gronenborn, A. M. *Biochemistry* **1989**, *28*, 7241-7257.

(74) Enari, T. M.; Niku-Paavola, M. L. *CRC Crit. Rev. Biotechnol* **1987**, *5*, 67-87.

(75) Ross, P.; Mayer, R.; Weinhouse, H.; Amikam, D.; Huggirat, Y.; Benziman, M.; de Vroom, E.; Fidder, A.; de Paus, P.; Sliedregt, L. A. J. M.; van der Marel, G. A.; van Boom, J. H. *J. Biol. Chem.* **1990**, *265*, 18933-18943.

(76) Haigler, C.; Brown, M. R.; Benziman, M. *Science* **1980**, *210*, 903-905.

(77) Quader, H.; Robinson, D. G.; van Kemp, R. *Planta* **1983**, *157*, 317-323.

(78) Kai, A.; Kitamura, H. *Bull Chem. Soc. Jpn.* **1985**, *58*, 2860-2862.

(79) Kai, A. *Makromol. Chem. Rapid Commun.* **1984**, *5*, 307-310.

(80) Kai, A.; Kido, H.; Ishida, N. *Chem. Lett.* **1990**, 949-952.

(81) Kai, A. *Makromol. Chem. Rapid Commun.* **1991**, *12*, 15-18.

(82) Haigler, C. H.; Chanzy, H. *Journal of Ultrastructure and Molecular Structure Research* **1988**, *98*, 299-311.

(83)   Mizuta, S.; Brown, J. R. M. *Protoplasma* **1992**, *166*, 200-207.

(84)   Wood, P. J. *Carbohydrate Res.* **1981**, *94*, C19-C23.

(85)   Ritcey, A. M.; Gray, D. G. *Biopolymers* **1988**, *27*, 479-491.

(86)   Hatano, M. *Induced Circular Dichroism in Biopolymer-Dye Systems*; Springer-Verlag:Berlin, 1986; Vol. 77.

(87)   Yalpani, M. *Polysaccharides*; Elsevier:Amsterdam, 1988.

(88)   Buchanan, C. M.; Hyatt, J. A.; Kelley, S. S.; Little, J. L. *Macromolecules* **1990**, *23*, 3747-3755.

(89)   Haigler, C. H. Ph. D. Thesis, University of North Carolina, Chapel Hill, 1982.

(90)   Benesi, H. A.; Hildebrand, J. H. *J. Am. Chem. Soc.* **1949**, *71*, 2703-2707.

(91)   Han, S. M.; Purdie, N.; Swallows, K. A. *Anal. Chim. Acta* **1987**, *197*, 57-64.

(92)   Ben-Naim, A. *Hydrophobic Interactions*; Plenum Press:New York, 1980.

(93)   Spurlino, J. C.; Lu, G.; Quiocho, F. A. *J. Biol. Chem* **1990**, *266*, 5202-5219.

(94)   Quiocho, F. A. *Pure Appl. Chem.* **1989**, *61*, 1293-1306.

(95)   Quiocho, F. A.; Nand, K. *Nature* **1984**, *310*, 381-386.

(96)   Vyas, N. K.; Vyas, M. N.; Quiocho, F. A. *Science* **1988**, *242*, 1290-1295.

(97)   Shieh, W. J.; Tsai, G. J.; Ladisch, M. R.; Tsao, G. T. *Appl. Biochem. Biotechnol.* **1989**, *22*, 13-29.

(98)   Van Tilbeurgh, H.; Loontiens, F. G.; Engelborgs, Y.; Claeyssens, M. *Eur. J. Biochem.* **1989**, *184*, 553-559.

(99)   Alurralde, J. L.; Ellenrieder, G. *An. Asoc. Quim. Argent.* **1985**, *73*, 231-237.

(100) *The Structures of Cellulose*; Atalla, R. H., Ed.; American Chemical Society: 1985; Vol. 340.

(101) Taiz, L.; Zeiger, E. *Plant Physiology*; The Benjamin/Cummins Publishing Company, Inc.:Redwood City, California, 1991.

(102) *The Flavonoids, Advances in Research Since 1986*; Harborne, J. B., Ed.; Chapman & Hall:London, 1994.

(103) Dixon, R. A.; Choudhary, A. D.; Dalkin, K.; Edwards, R.; Fahrendorf, T.; Gowri, G.; Harrison, M. J.; Lamb, C. J.; Loake, G. J.; Maxwell, C. A.; Orr, J.; Paiva, N. L. In *Phenolic Metabolism in Plants*; H. A. Stafford and R. K. Ibrahim, Eds.; Plenum Press:New York, 1992.

(104) Strange, R. N.; Ingham, J. L. *Z. Naturforsch* **1985**, *40c*, 313-316.

(105) VanEtten, H. D.; Matthews, D. E.; Matthews, P. S. *Annu. Rev. Phytopathol.* **1989**, *27*, 143-164.

(106) VanEtten, H. D.; Matthews, P. S.; Mercer, E. H. *Phytochemistry* **1983**, *22*, 2291-2295.

(107) Dixon, R.; Paiva, N. L.; Edwards, E.; Sun, Y.; Hrazdina, G. *Plant Molecular Biology* **1991**, *17*, 653-667.

(108) Paiva, N. L., Personal Communication.

(109) Schöning, A.; Friedrichsen, W. *Z. Naturforsch* **1989**, *44b*, 975-982.

APPENDIX A

METHOD FOR CALCULATION OF EQUILIBRIUM CONSTANTS
OF 1:1 ASSOCIATION COMPLEXES

The algorithm for the calculation of association constants was adapted from the graphical method used by Benesi and Hildebrand.[90]

For the reaction:

$$D + S \leftrightarrow DS \tag{1}$$
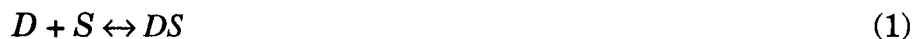
where D, S, and DS are defined as the dye, sugar, and 1:1 association complex, respectively.

The expression for the equilibrium constant is given by

$$K = \frac{[DS]}{[D][S]} \tag{2}$$

where [ ] indicates the equilibrium concentrations of the respective species.

The analytical concentrations for the dye and sugar, C_D and C_S, are

$$C_D = [D] + [DS] \tag{3}$$

$$C_S = [S] + [DS] \tag{4}$$

Solving (3) and (4) for $[D]$ and $[S]$ and substituting into (2) gives

$$K_{DS} = \frac{[DS]}{(C_D - [DS])(C_S - [DS])} \qquad (5)$$

since, according to Beer's law,

$$\psi = \theta_{DS} b [DS] \qquad (6)$$

where ψ is the measured ellipticity in mdeg, θ_{DS} is the molar ellipticity, and b is the path length in cm.

Solving (6) for [DS] and substituting into (5) yields

$$K_{DS} = \frac{\psi/b\theta_{DS}}{\left(C_D - [DS]\right)\left(C_S - [DS]\right)} \qquad (7)$$

Upon rearrangement, (7) gives

$$(C_D - [DS])(C_S - [DS]) = \frac{\psi}{\theta_{DS} K_{DS} b} \qquad (8)$$

Multiplying and rearranging in (8) gives

$$[DS](C_D + C_S - [DS]) = C_D C_S - \frac{\psi}{\theta_{DS} K_{DS} b} \qquad (9)$$

Substituting for [DS] as in step (7) gives

$$\frac{\psi}{\theta_{DS} b}(C_D + C_S - [DS]) = C_D C_S - \frac{\psi}{\theta_{DS} K_{DS} b} \qquad (10)$$

Multiplying by ψ/b and rearranging gives the linear expression in the form $y=mx + b$

$$\frac{bC_DC_S}{\psi} = \frac{C_D + C_S - [DS]}{\theta_{DS}} + \frac{1}{K_{DS}\theta_{DS}} \qquad (11)$$

where $m = \frac{1}{\theta_{DS}}$ and $b = \frac{1}{K_{DS}\theta_{DS}}$.

Since both K_{DS} and θ_{DS} are unknown, the calculation must be done by an iterative process, which typically starts with a value of $[DS]=0$. The $[DS]$ is approximated successively and K_{DS} is calculated by taking the ratio of the slope to the intercept. The iteration is terminated when successive K values differ by a predetermined amount, in this case ± 10. A short computer program was written in the BASIC language using Cramer's Rule[34] to provide the least squares solution. This program was later converted to a Hypercard® stack to facilitate its use on a Macintosh™ personal computer.

VITA

Allan Ray Engle

Candidate for the Degree of

Doctor of Philosophy

Thesis: ANALYTICAL APPLICATIONS OF CIRCULAR DICHROISM: USE OF COLOR INDUCTION REACTIONS FOR QUALITATIVE AND QUANTITATIVE ANALYSIS

Major Field: Chemistry

Biographical:

>   Personal Data: Born in Waynoka, Oklahoma, on May 17, 1958, the son of Donald and Lena Faye Engle.

>   Education: Graduated from Waynoka High School, Waynoka, Oklahoma, May 1976. B.S. in Education, Northwestern Oklahoma State University, May 1981. B.A. in Chemistry, Southwestern Oklahoma State University, May 1986. M.S. in Chemistry, Oklahoma State University, May 1990. Completed requirements for the Doctor of Philosophy in Chemistry at Oklahoma State University in July 1994.

>   Professional Experience/Honors: Eastman Kodak Research Assistantship, 1991-present. Research Collaboration, The Noble Foundation, Division of Plant Pathology, 1991-present. Centennial Research Excellence Award, Oklahoma State University, 1990. Instructor, Kerr Scholars, Oklahoma State University, 1989 & 1990. Burroughs-Wellcome Research Assistantship, 1988-present. Instructor, Young Scholars: Futures in Science, 1988. Graduate Teaching Assistant, Oklahoma State University, 1987-present. Chemistry Storeroom Manager, Southwestern Oklahoma State University, 1986-87. Teaching Assistant, Southwestern Oklahoma State University, 1985-87. Instructor, Upward Bound, Southwestern Oklahoma State University, 1985-86. Science Instructor, Shidler High School, 1983-84. Science Instructor, Freedom High School, 1981-83.

>   Professional Membership: American Chemical Society.